A SOLUTION TO THE KERMACK AND MCKENDRICK INTEGRO-DIFFERENTIAL EQUATIONS WHICH ACCURATELY PROJECTS COVID-19 CASE DATA USING GOOGLE MOBILITY DATA AS AN INPUT

Ted Duclos, Tom Reichert

Author affiliations:

T. Duclos, Ted Duclos Advisors, St. Augustine, Florida, ORCID: 0000-0002-5623-2623, email address: tedduclos56@gmail.com

T. Reichert, Entropy Research Institute, Portland, Oregon. ORCID: 0000-0003-3006-5385

Author contributions: T. Duclos and T. Reichert: Conceptualization, Writing – Original draft preparation, Writing – Review & Editing. T. Duclos: Methodology, Validation. T. Reichert: Data Investigation.

Funding: This work received no specific funding.

Declarations of interest: none.

Word counts: Abstract, 240 words; text, 10,090 words

Key Words

Kermack and McKendrick integro-differential equations

Closed form solution

Epidemic management

Covid-19 Projections with Google Residential Mobility Measure

Abbreviations used in this text

KMES	Kermack McKendrick integro-differential Equation Solution
RCO	Rate of Change Operator
SIR	Susceptible–Infectious–Recovered

Abstract

In this manuscript, we derive a closed form solution to the full Kermack and McKendrick integro-differential equations (Kermack and McKendrick 1927) which we call the KMES. We demonstrate the veracity of the KMES using the Google Residential Mobility Measure to accurately project case data from the Covid 19 pandemic and we derive many useful, but previously unknown, analytical expressions for characterizing and managing an epidemic. These include expressions for the viral load, the final size, the effective reproduction number, and the time to the peak in infections. The KMES can also be cast in the form of a step function system response to the input of new infections; and that response is the time series of total infections.

Since the publication of Kermack and McKendrick's seminal paper (1927), thousands of authors have utilized the Susceptible, Infected, and Recovered (SIR) approximations; expressions putatively derived from the integro-differential equations to model epidemic dynamics. Implicit in the use of the SIR approximation are the beliefs that there is no closed form solution to the integro-differential equations, and that the approximation is a special case which adequately reproduces the dynamics of the integro-differential equations mapped onto the physical world. However, the KMES demonstrates that the SIR approximations are not adequate representations of the integro-differential equations, and we therefore suggest that the KMES obsoletes the need for the SIR approximations by providing not only a new mathematical perspective, but a new understanding of epidemic dynamics.

Introduction

Modern epidemiological modeling has its roots in the Kermack and McKendrick epidemic model, first published in 1927 (Kermack and McKendrick 1927). Since its publication, well over 10,000 authors have referenced and used this paper as a foundational starting point. However, as Diekmann points out in his insightful essay (2022 pg. 8), "…an incessant community-enforced misconception is that the paper is just about the very special case, the S-I-R (Susceptible, Infected, Recovered) model." In the essay, he also elaborates on his suspicion that, despite the many references, the 1927 paper is rarely read by the citing authors. His concluding remarks decry the situation and request that the 1927 paper, a "…true gem…in which tremendous wisdom lies hidden." (Diekmann 2022 pg. 9) be thoroughly read and mined for its insights.

In the setting of Diekmann's comments, we have found two broad themes throughout the epidemic literature that references Kermack and McKendrick's 1927 paper:

1) The SIR model approximation and its variants are accepted as a special case of the full equations (Kermack and McKendrick 1927, Breda et al 2021, Diekmann 2022 and Brauer 2008).

2) There are no known or published closed-form solutions to the full set of Kermack and McKendrick's integro-differential equations as evidenced by Diekmann (2021), wherein

the authors present a discrete-time model of the integro-differential equations. If a closed form solution exists, there is no need for such a model.

In view of these themes, we strongly support Diekmann's comments and suggest that the "generalizations" highlighted by Diekmann, wherein authors further develop the SIR special case, potentially take unknown mathematical risks when assuming that the base SIR model faithfully approximates the essence of the integro-differential equations. We point to the 1927 paper where a close reading reveals that Kermack and McKendrick justify the SIR approximation by summarily substituting two constants for their two key parameters: a stark contrast to their careful construction of the integro-differential equations themselves. The resulting SIR approximation inherently assumes that the affected population is well mixed, an assumption rightly pointed out as "unrealistically simple" in the literature (Brauer 2008, pg. 27); and this begs the question: is this a warning sign that the approximation may be lacking in fidelity to the full equations? Therefore, as Diekmann's essay seems to suggest, is it not logical to choose the integro-differential equations as a starting point to develop generalizations?

We ask these questions because we assert, for instance, that a solution of Kermack and McKendrick's integro-differential equations themselves need not depend on the assumption of a well-mixed population. As we show in this manuscript, starting with their integro-differential equations, they can be solved using an equivalent set of expressions that do not invoke the well-mixed assumption.

We also respectfully note here that network-based stochastic models (e.g., Newman, m. 2002, Diekmann, O et al, 1998, and Youssef, M, 2011), operating on the assumption that epidemic dynamics can be projected by summing the collective probabilities of individuals being infected by their contacts, have been widely investigated as an alternative to the well-mixed assumption. These have even been used to develop estimations of outbreak threshold conditions and final sizes of epidemics. However, while these are logical steps towards the use of more realistic characteristics of interactions, a significant drawback of all these refinements is that they do not yield closed-form analytical expressions describing the course of an epidemic. We therefore ask, as suggested by Diekmann's essay: would an analytical solution to the integro-differential equations yield significantly more insight, even wisdom, about epidemic dynamics?

In this manuscript, we address these questions and Diekmann's call to action in three sections:

1) In Section 1 we derive an analytical solution to the Kermack and McKendrick integro-differential equations by first recasting the equations and then applying a mean field approximation. This allows the solution to be expressed in terms of two parameters: 1) transmissibility and 2) population interaction. We call the solution the KMES (**K**ermack and **M**cKendrick **E**quation **S**olution). From the KMES, we derive and explicate many analytical expressions characterizing epidemic dynamics such as final size, the basic and effective reproduction number, the time to peak new infections and the number of infections at the peak.

2) In Section 2, using the data compiled from several countries during the COVID-19 pandemic, we then demonstrate that the transmissibility, normalized viral load, and population interaction parameters can be deduced in a straightforward manner from early pandemic data together with the independently sourced Google Residential Measure (Google 2023). We use these values and the KMES to accurately project the course of the Covid-19 pandemic in six sampled countries.

3) In Section 3 we derive additional expressions which can be used to determine the actions necessary to control and end an epidemic. We demonstrate the use of these expressions with the United States Covid-19 case data from March 2020 to November 2021.

Within each of these sections, as the opportunity arises, we contrast the epidemic dynamics projected by the KMES against those projected by a representative SIR model. In these instances, we find the SIR model lacking in fidelity to important dynamics found in the data.

Section 1: Solution to the Kermack and McKendrick Equations

(Note: We use the following equation notation, (X, SY-Z), where X is the equation number in the body; and if the equation is used in a supplement, Y is the supplement number and Z is the number of the equation in the supplement). A list of all equations is provided in Supplement 5.

Definition of Terms

We begin by defining several quantities to describe epidemic dynamics. These are: N_P, the total population of people who can become infected during the epidemic; $S(t)$, the subpopulation that

has not yet become infected; $N(t)$, the subpopulation that is currently or has previously been infected; $I(t)$, the infectiousness of individuals within $N(t)$; and $\mathrm{R}(t)$, the total recovery of individuals within $N(t)$. The relationships among these quantities are further clarified by noting that $S(0)$ is the number of uninfected people in N_P at the epidemic start, $S(\infty)$ is the number of uninfected people at the end of the epidemic, $I(0)$ is the number of infectious individuals at the epidemic start; and therefore, $N_P = S(t) + N(t)$, $N(t) = I(t) + R(t)$, and $N(0) = I(0)$. We further assume that for our modelling purposes, N_P is a constant and that once infected, people cannot become reinfected.

As defined, $I(t)$ is the infectiousness of the population $N(t)$ where, by "infectiousness", we mean the ability to infect others. Also, as defined, $R(t)$ is the portion of $N(t)$ that is unable to infect others and is therefore "not infectious". To avoid any ambiguities in these definitions, we clarify them further using three thought experiments.

In the first thought experiment, we imagine a person with an active infection who has no contact at all or contact only with persons who cannot become infected. This person is certainly a member of the ever-infected population $N(t)$; but since they cannot infect anyone, they cannot advance the epidemic. Therefore, they are not included in expressions for the number who are infectious; but rather, they are included in $R(t)$.

In a second thought experiment, imagine that a person has just infected a particular person. In this case, the infecting person cannot reinfect that newly infected person nor can the newly infected person infect their infector. In our model, we assume that the frequency and

number of interactions between people does not change quickly when compared to the rate at which people become infected. Consequently, we assume that the infectors remain somewhat durably in infectious contact with the people they have infected. Therefore, according to our assumptions, the infectiousness of infectors diminishes with each infection they cause; and, in symmetry, the degree to which they are unable to infect others, their recovery, increases.

In the third thought experiment, as described in Diekmann (2022), during an infection, the quantity and quality of the infectious agent within any infected person, the so-called "viral load", will rise and fall with time. Since the potential of a person to infect susceptible people will also vary in synchrony, we postulate that the level of infectiousness will approximately track the variation in viral load. It is easy to see that those persons whose infection has passed the maximum viral load will become increasingly less infectious; and, correspondingly more recovered. We say "approximately" when discussing the relationship of infectiousness to decreasing viral load, because infectiousness and viral load are not equivalent, as the notions developed in the first and second thought experiments make clear.

Within these definitions and, as illustrated by the three thought experiments, the key characteristic is that $I(t)$ is a measure of infectiousness dependent upon a person's ability and, importantly, opportunity to infect others. This leads inexorably to the conclusion that the membership of an individual will necessarily sometimes be split between the $I(t)$ and $R(t)$ subpopulations. An appreciation of this shared membership is critical to the interpretation of the solution that emerges below.

Our Approach to the Solution

The following relationship is a common starting point in epidemic models (Breda et al, 2021; Diekmann et al, 2021),

$$\frac{dS(t)}{dt} = -\frac{dN(t)}{dt} = -\Lambda(t)S(t), \quad (1)$$

where $\Lambda(t)$ is known as the force of infection and is the product of the disease transmissibility (often designated as $\beta(t)$) and $\mathrm{I}(t)$. This equation can be deduced from one of Kermack and McKendrick's original equations.

The motivation behind this starting point is that the problem is usually formulated as the need to track the number of originally susceptible people who become infected and, in the process, determine the remaining number of people who never become infected. Unfortunately, by defining the problem this way and by choosing Equation 1 as the starting point, a modeler implicitly makes the critical assumption that $\mathrm{S}(t) > 0$ before Equation 1 can be solved. This assumption biases the number and nature of potential solutions and, therefore, we submit it should be avoided if possible.

(Authors' note: we acknowledge that allowing the possibility that $S(t) = 0$ is a violation of the accepted tenet that herd immunity is an inherent property of the Kermack and McKendrick model. We point out, however, that allowing the possibility that $S(t) = 0$ simply requires that the force of infection approaches infinity as $S(t) \to 0$. Of course, $I(t)$ can never be infinite,

however, since the units of $\beta(t)$ are $\frac{new\ infections}{(infected\ x\ susceptible\ x\ time)} = \frac{1}{(susceptible\ x\ time)}$, it, as well as the force of infection, will surely approach infinity as $S(t) \to 0$.)

As an alternative to the conventional start, we begin our development with a complementary relationship,

$$-\frac{dS(t)}{dt} = \frac{dN(t)}{dt} = K_T(t)I(t), \tag{2}$$

where $K_T(\mathrm{t})$ is a function describing the rate of new infections. Equation 2 arises from the notion that the currently infectious subpopulation, $I(t)$, is the sole cause of new infections. This is a "systems" view, in which infections are expressly recognized as the source of all new infections. We also note that Equation 2 does not impose any restrictions on the range of the variables involved other than the logical restriction that all population totals must always be non-negative.

A solution to Equation 2 can be found by first writing the additional relationship,

$$\frac{dI(t)}{dt} = (K_T(t) - \mu(t))I(t), \tag{3}$$

where $\mu(t)$ is the recovery rate of the infected people. Equation 3 is then easily solved for $\mathrm{I}(t)$,

$$I(t) = I(0)e^{\int_0^t (K_T(b) - \mu(b))db}. \tag{4}$$

Using Equation 4, we can subsequently solve Equation 2 for $\mathrm{N}(t)$,

$$N(t) = \int_0^t K_T(\mathrm{c})\mathrm{I}(0)\, e^{\int_0^c (K_T(b) - \mu(b))db} dc \tag{5}$$

with the logical restriction that $N(t) \leq S(0)$.

We now introduce the Kermack and McKendrick model and demonstrate that Equations 2 and 3 are expressions equivalent to the full Kermack and McKendrick integro-differential equations. This leads us to the KMES.

Kermack and McKendrick's model structure

Kermack and McKendrick (1927) derived their integro-differential equations by imagining $N(t)$ as the sum of incremental subpopulations which had been infected at the time $t - \theta$; where θ is the time since infection of each subpopulation. The time history of the epidemic was then imagined as a t-by-t array with every successive row representing an increment of time, Δt, and each column representing an increment of θ. In our rendition of the model, since θ has the units of time, we designate each increment of θ as Δt, and note that the array is square because $\theta \leq t$; and $\Delta\theta = \Delta t$.

The progress of each θ group in Kermack and McKendrick's analysis was tracked through time across the array with each θ group starting at time $t - \theta$ and progressing diagonally thereafter. Their equations were then developed by summing over θ and then taking the limit as $\Delta\theta$ and $\Delta t \to 0$. To assist in understanding the relationship between time and θ, a complete rendition of the arrays underpinning their equations is presented in Supplement 5.

We adopt Kermack and McKendrick's equations θ convention and adapt the format of their equations using the following notation. In our notation, unless otherwise specified, all dependent variables and parameters are assumed to depend on both time, t, and θ (e.g., $I(t, \theta)$ or

$\psi(t,\theta)$). If a variable (not a parameter) is designated as a function of time alone, then it is to be understood that the variable has been integrated over all θ. For instance, $I(t) = \int_0^t I(t,\theta)\, d\theta$. In contrast to the variables, however, if we designate a parameter as solely a function of time or θ, then the parameter is to be considered constant over the alternate temporal dimension; i.e, θ or time respectively. The dependent variables used in this manuscript are S, I, N, and R; and the parameters are: K_T, P_c, φ, φ_r, ρ, ψ, μ, β, P_{cr}, and γ.

We also note that Kermack and McKendrick, in their manuscript (1927), expressed the parameters, φ and ψ, in different positions within their equations as solely dependent on either θ or t, which is sometimes confusing. For clarity, we choose to initially show these parameters as dependent on both θ and t (i.e., we write them as $\varphi(t,\theta)$ and $\psi(t,\theta)$); and then let the analysis determine whether they are solely dependent on θ, t, or both. It develops that this heightened level of precision is necessary to resolve what would otherwise be ambiguities.

With the conceptualizations developed above, we now write the Kermack and McKendrick integro-differential equations in terms of time, θ, and our dependent variables:

$$\frac{dS(t)}{dt} = -\frac{S(t)}{A_p}\left(\int_0^t A(t,\theta)\frac{dN(t-\theta,0)}{dt}\, d\theta + A(t,t)I(0)\right), \tag{6}$$

$$I(t) = \int_0^t B(t,\theta)\frac{dN(t-\theta,0)}{dt}\, d\theta + B(t,t)I(0), \tag{7}$$

$$\frac{dR(t)}{dt} = \int_0^t C(t,\theta)\frac{dN(t-\theta,0)}{dt}\, d\theta + C(t,t)I(0), \tag{8}$$

$$N(t) = I(t) + R(t) \tag{9}$$

where $B(t,\theta) = e^{-\int_{t-\theta}^{t}\psi(t,a)da}$, $C(t,\theta) = \psi(t,\theta)B(t,\theta)$, and $A(t,\theta) = \varphi(t,\theta)B(t,\theta)$. Kermack and McKendrick (1927, p. 703) defined $\varphi(t,\theta)$ as "the rate of infectivity at age θ", and $\psi(t,\theta)$ as "the rate of removal" of the infected population to the recovered population. A_p is the area that contains the population and, as previously defined, θ is the time since infection of any member of the population $N(t)$.

The integration limits in the expression for $B(t,\theta)$ are a critical feature, and, therefore, deserve special attention. In the development of their equations, Kermack and McKendrick assumed that the B term, the infectiousness of each θ group at time, t, was only a function of θ because they assumed that every θ group would begin and then proceed along identical time paths of infectiousness. Consequently, in their manuscript, the integration limits in the B term were chosen to only depend upon the time since infection (i.e., 0 to θ), regardless of the actual time interval. They could have been more precise in their notation. As we show in our definition of $B(t,\theta)$, the precise integration limits are $t-\theta$ and t, the actual time interval associated with each θ group. This time interval also has length θ, as in Kermack and McKendrick's original formulation.

The specification of the proper integration limits is critical to obtaining and demonstrating the solution because, as we show in what follows, the fraction of people in the contacts of $\mathrm{I}(t)$ that have already been infected is dependent on the actual time. Therefore, the infectiousness of each θ group is also dependent on the actual time, not solely the time since infection. This is determinant in the path to a closed form.

Derivation of the KMES

Because the path to deriving the KMES is complex, we summarize the steps in the following list as a guide:

1. We first rewrite Equations 6 through 9 solely in terms of time by defining two parameters, $\mu(t)$ and $K_T(t)$ as the weighted averages of functions of $\varphi(t,\theta)$ and $\psi(t,\theta)$ respectively.

2. We then find the general solution to these rewritten equations and confirm the form of the relationships between $\mu(t)$ and $K_T(t)$ and between $\varphi(t,\theta)$ and $\psi(t,\theta)$.

3. With these relationships in hand, we then proceed to derive an equation describing the effect of the population interactions, defined as $P_c(t)$, on the evolution of the fraction of ever infected people that are still infected.

4. This equation is then used to find the final form of the KMES by expressing it and all the parameters of the Kermack and McKendrick integro-differential equations in terms of $K_T(t)$ and $P_c(t)$ which represent the disease transmissibility and the population interactions respectively.

Step 1: Rewrite the integro-differential equations

We begin rewriting and solving Equations 6 through 9 by using the definition of $N(t)$ as the total number of people that have been infected. Therefore:

$$N_P - S(t) = N(t) \tag{10}$$

and,

$$\frac{dS(t)}{dt} = -\frac{dN(t)}{dt} \tag{11}$$

We now restate Equation 2,

$$-\frac{dS(t)}{dt} = \frac{dN(t)}{dt} = K_T(t)I(t), \tag{2}$$

and we remark that it describes a direct relationship between the cause of the epidemic, the infections, and the change in the susceptible population. From its form, the units of $K_T(t)$ must be: $\frac{New\ Infections}{Infected\ person\ x\ Time}$ meaning that it is a transmission rate. This equation embodies the notion that, from a systems standpoint, all the new infections must be caused by contact with the currently infectious.

If we divide Equation 6 by Equation 7, and combine the result with Equation 2, we can express $K_T(t)$ in terms of Kermack and McKendrick's variables as,

$$K_T(t) = -\frac{\frac{dS(t)}{dt}}{I(t)} = \frac{\mathrm{S(t)}\left(\int_0^t A(t,\theta)\frac{dN(t-\theta,0)}{dt}d\theta + A(t,t)I(0)\right)}{A_P\left(\int_0^t B(t,\theta)\frac{dN(t-\theta,0)}{dt}d\theta + B(t,t)I(0)\right)}. \tag{12}$$

Likewise, by dividing Equation 8 by Equation 7 we can also define $\mu(t)$ as,

$$\mu(t) = \frac{\frac{dR(t)}{dt}}{I(t)} = \frac{\int_0^t C(t,\theta)\frac{dN(t-\theta,0)}{dt}d\theta + C(t,t)I(0)}{\int_0^t B(t,\theta)\frac{dN(t-\theta,0)}{dt}d\theta + B(t,t)I(0)}. \quad (13)$$

We note here that, for a given time, t, as θ goes from 0 to t, $\mu(t)$ is defined as the weighted average of $\psi(t,\theta)$ and $K_T(t)$ as the weighted average of $\varphi(t,\theta)\frac{S(t)}{A_p}$.

We then rewrite Equations 6 through 9 in the following form,

$$-\frac{dS(t)}{dt} = \frac{dN(t)}{dt} = K_T(t)\, I(t), \quad (14)$$

$$\frac{dI(t)}{dt} = K_T(t)\, I(t) - \mu(t)\, I(t), \quad (15)$$

$$\frac{dR(t)}{dt} = \mu(t) I(t) \text{ and} \quad (16)$$

$$S(t) = N_P - N(t), \quad (17)$$

where $N(t) = I(t) + R(t)$. As heralded in the introduction, these equations do not require that the population be well mixed or specify any level of mixing, and, consequently, later in the derivation, we introduce a population interaction term.

Step 2. Solve the rewritten equations

We recognize Equations 14 and 15 as Equations 2 and 3, therefore, their solutions are Equations 4 and 5,

$$N(t) = \int_0^t K_T(c) I(0)\, e^{\int_0^c (K_T(b) - \mu(b))db} dc \quad (5)$$

$$I(t) = I(0) e^{\int_0^t (K_T(b) - \mu(b))db} \quad (4)$$

The task remains to determine the requirements of $K_T(t)$ and $\mu(t)$ in which Equations 4 and 3 also solve Equations 6 through 9. We accomplish this by first recalling that $K_T(t)$ and $\mu(t)$ are defined as the weighted averages of $\varphi(t,\theta)\frac{S(t)}{A_p}$ and $\psi(t,\theta)$ respectively. We then take $K_T(t) = \varphi(t,\theta)\frac{S(t)}{A_p}$ and $\mu(t) = \psi(t,\theta)$ as an ansatz, and recognize that $\frac{dN(t)}{dt} = \frac{dN(t,0)}{dt}$, since the value of $\frac{dN(t,\theta)}{dt} = 0$ for all $\theta > 0$. Then, noting that Equation 2 defines the relationship between $\frac{dN(t)}{dt}$ and $I(t)$, we can substitute Equations 4 and 2 into Equations 6 and 7, while utilizing the exponential forms of $B(t,\theta)$ and $B(t,t)$ (keeping in mind that $d\theta = dt$), to show that if the ansatz $K_T(t) = \varphi(t,\theta)\frac{S(t)}{A_p}$ and $\mu(t) = \psi(t,\theta)$ is true, then Equations 5 and 3 are indeed solutions to Equations 6 through 7. We leave this to the reader to follow the steps and prove this to themselves.

Step 3: Define the effect of the population interactions

Although Equations 4 and 5 are mathematical solutions to the integro-differential equations, they can only project the course of an epidemic if we can evaluate the parameters $K_T(t)$ and $\mu(t)$ a priori. To satisfy this need, and, since Kermack and McKendrick did the same, we first hypothesize that there are but two free parameters: one describing the disease transmission and the other describing the interactions of the population.

Since $K_T(t)$, was already introduced as the rate of disease transmission from infectious people to newly infected people, we assume that it is the parameter describing disease transmission and thus can be found in the disease or epidemic data. While we initially make this

assumption based on the structure of the equations, this assumption is fully supported in Section 2 by the data from the Covid-19 pandemic.

To describe the population interaction, we define a second parameter, $P_c(t)$:

$$P_c(t) = \lim_{\Delta t \to 0} \int_t^{t+\Delta t} P_{cr}(t)dt, \tag{18}$$

where $P_{cr}(t)$ is the average rate of infectious contact for the entire population. Consequently, $P_c(t)$ is understood to be the instantaneous average number of contacts within the population. Infectious contacts are allowed to be fractions of a whole between two contacts; or, in other words, there is an amplitude associated with every contact; and these weighted contacts average to $P_c(t)$ for the population. This is equivalent to a mean field approximation of the population interactions.

Having defined our two plausibly measurable parameters as $K_T(t)$ and $P_c(t)$, we continue the analysis by noting that every person within both $N(t)$ and $I(t)$ contacts $P_c(t)$ people in each period Δt. In accordance with Equation 2 and beginning at $t = 0$, $K_T(0)I(0)\Delta t$ people within the $I(0)P_c(0)$ group then become infected during the period from 0 to Δt. Concurrently, the number of non-infected people within the $I(0)P_c(0)$ group is reduced to $I(0)P_c(0) - K_T(0)I(0)\Delta t + I(0)\Delta P_{cni}(0)$; where $P_{cni}(t)$ is defined as the number of people within $P_c(t)$ who are still susceptible. We add the term $I(0)\Delta P_{cni}(0)$ to account for any additional susceptible people that the $I(t)$ group may contact infectiously during the time interval Δt.

Therefore, since $\frac{K_T(0)\Delta t}{P_c(0)}$ is the portion of $P_c(0)$ the contacting infected people can no longer infect and $\frac{\Delta P_{cni}(0)}{P_c(0)}$ is the number of new contacts that can be infected, per potentially infectious contact, $I(0)P_c(0)$, the infectiousness of the people within $N(0)$, has been changed by the factor, $1-\frac{K_T(0)\Delta t-\Delta P_{cni}(0)}{P_c(0)}$. After a time Δt, the infectiousness, $I(\Delta t)$, per contact, in the affected population $N(\Delta t)$ is,

$$I(\Delta t)=N(\Delta t)-\frac{K_T(0)\Delta t-\Delta P_{cni}(0)}{P_c(0)}N(\Delta t). \tag{19}$$

Dividing both sides by $N(\Delta t)$, we obtain a difference equation for the ratio of the infectiousness, $I(\Delta t)$, to the total of the ever-infected population, $N(\Delta t)$,

$$\frac{I(\Delta t)}{N(\Delta t)}=1-\frac{K_T(0)\Delta t-\Delta P_{cni}(0)}{P_c(0)} \tag{20}$$

During the next time step, another $K_T(\Delta t)\Delta t I(\Delta t)$ people within the group $P_c(\Delta t)$ become infected and the infectiousness within $N(2\Delta t)$ is changed by an additional factor, $1-\frac{K_T(\Delta t)\Delta t-\Delta P_{cni}(\Delta t)}{P_c(\Delta t)}$. This is expressed mathematically as,

$$\frac{I(2\Delta t)}{N(2\Delta t)}=\left(1-\frac{K_T(0)\Delta t-\Delta P_{cni}(0)}{P_c(0)}\right)\left(1-\frac{K_T(\Delta t)\Delta t-\Delta P_{cni}(\Delta t)}{P_c(\Delta t)}\right). \tag{21}$$

The process repeats itself in each period Δt; and we can write,

$$\frac{I(n\Delta t)}{N(n\Delta t)}=\left(1-\frac{K_T(0)\Delta t-\Delta P_{cni}(0)}{P_c(0)}\right)\left(1-\frac{K_T(\Delta t)\Delta t-\Delta P_{cni}(\Delta t)}{P_c(\Delta t)}\right)\ldots\left(1-\frac{K_T(n\Delta t)\Delta t-\Delta P_{cni}(n\Delta t)}{P_c(n\Delta t)}\right). \tag{22}$$

Applying the second thought experiment, we now make the simplifying assumption that a change, $\Delta P_{cni}(t)$, to $P_{cni}(t)$ will occur much more slowly than the creation of new infections, which means that $\Delta P_{cni}(n\Delta t) \ll K_T(n\Delta t)\Delta t$. Therefore, in Equation 22, we decide to neglect the $\Delta P_{cni}(n\Delta t)$ terms. (A situation where $\Delta \mathrm{P_{cni}(n\Delta t)}$ is plausibly growing as fast as $\mathrm{K_T(n\Delta t)\Delta t}$ indicates an outbreak from the initial epidemic and is explored further in Supplement 3.1.)

Neglecting the $\Delta P_{cni}(n\Delta t)$ terms in Equation 22; and, since by definition, $n\Delta t = t$, as $n \to \infty, \Delta t \to 0$, Equation 22 becomes,

$$\frac{I(t)}{N(t)} = F_i(0)e^{-\int_0^t \frac{K_T(t)}{P_c(t)}dt}, \tag{23}$$

where $F_i(0) = \frac{I(0)}{N(0)}$; the fraction of $N(t)$ infected at $t = 0$. Equation 23 is the expression that enables us to complete the solution.

Step 4: The KMES

By dividing Equation 2 by $N(t)$, integrating, and exponentiating we obtain,

$$N(t) = N(0)e^{\int_0^t K_T(t)\frac{I(t)}{N(t)}dt}. \tag{24}$$

When Equation 23 is substituted into Equation 24, we find $\mathrm{N(t)}$,

$$N(t) = N(0)e^{F_i(0)\int_0^t K_T(t)e^{-\int_0^t \frac{K_T(a)}{P_c(a)}da}dt}. \tag{25}$$

We then find $I(t)$ by multiplying Equations 24 and 25,

$$I(t) = I(0)e^{F_i(0)\int_0^t K_T(t)e^{-\int_0^t \frac{K_T(a)}{P_c(a)}da}dt - \int_0^t \frac{K_T(t)}{P_c(t)}dt}, \quad (26)$$

and from the definition of $N(t)$, using Equations 25 and 26 we find $R(t)$,

$$R(t) = (N(0) - I(0)e^{-\int_0^t \frac{K_T(t)}{P_c(t)}dt})e^{F_i(0)\int_0^t K_T(t)e^{-\int_0^t \frac{K_T(a)}{P_c(a)}da}dt}. \quad (27)$$

If we substitute Equations 25 to 27 into Equations 14 through 17, we find that $\mu(t) = K_T(t) - F_i(0)K_T(t)e^{-\int_0^t \frac{K_T(t)}{P_c(t)}dt} + \frac{K_T(t)}{P_c(t)}$, the sought after expression for $\mu(t)$.

As a check, we can then substitute this expression for μ(t) into Equations 3 and 4 and demonstrate their equivalency to Equations 25 and 26. We therefore conclude that Equations 25, 26, and 27 are solutions to Kermack and McKendrick's integro-differential equations in terms of the transmission and interaction parameters, $K_T(t)$ and $P_c(t)$.

To completely specify the solution to Kermack and McKendrick's integro-differential equations, in terms of $K_T(t)$ and $P_c(t)$ we now have,

$$B(t,\theta) = e^{-\int_{t-\theta}^t \psi(t,a)da} = e^{-\int_{t-\theta}^t (K_T(a) - F_i(0)K_T(a)e^{-\int_0^a \frac{K_T(b)}{P_c(b)}db} + \frac{K_T(a)}{P_c(a)})da} \quad (28)$$

$$B(t,t) = e^{-\int_0^t \psi(t,a)da} = e^{-\int_0^t (K_T(a) - F_i(0)K_T(a)e^{-\int_0^a \frac{K_T(b)}{P_c(b)}db} + \frac{K_T(a)}{P_c(a)})da} \quad (29)$$

$$\mu(t) = \psi(t,\theta) = \frac{\frac{dR(t)}{dt}}{I(t)} = K_T(t) - F_i(0)K_T(t)e^{-\int_0^t \frac{K_T(t)}{P_c(t)}dt} + \frac{K_T(t)}{P_c(t)} \quad (30)$$

$$\varphi(t,\theta) = \frac{K_T(t)A_p}{S(t)} \tag{31}$$

Equations 25 through 31 are the KMES and they are a solution to Equations 6 through 9.

Since $\psi(t,\theta)$ and $\varphi(t,\theta)$ are solely functions of time in Equations 30 and 31, we therefore continue this manuscript with the nomenclature, $\psi(t)$ and $\varphi(t)$. Lastly, with no loss of generality, since $S(t) = N_P - N(t)$, rather than portray the progress of the epidemic in terms of susceptibles, $S(t)$, we henceforth express it in terms of the total cases, $N(t)$, as in Equation 25.

Simplified expressions

The expressions for $N(t)$, $I(t)$, and $R(t)$ can be rewritten in simplified, more intuitive forms. The first of these is what we call the Step Response form, which is found by using the expression for $B(t,t)$ (Equation 29) to rewrite $N(t)$, $I(t)$, and $R(t)$ as,

$$I(t) = e^{\int_0^t K_T(t)dt} B(t,t) I(0) \tag{32}$$

$$N(t) = e^{\int_0^t (K_T(t) + \frac{K_T(t)}{P_c(t)})dt} B(t,t) \frac{I(0)}{F_i(0)} \tag{33}$$

$$R(t) = \left(\frac{e^{\int_0^t (K_T(t) + \frac{K_T(t)}{P_c(t)})dt}}{F_i(0)} - e^{\int_0^t K_T(t)dt}\right) B(t,t) I(0). \tag{34}$$

Since $B(t,t)$ is the time varying infectiousness input of the original infected group, $I(0)$, the exponential expressions, $e^{\int_0^t K_T(t)dt}$, $\frac{e^{\int_0^t (K_T(t) + \frac{K_T(t)}{P_c(t)})dt}}{F_i(0)}$, and $\frac{e^{\int_0^t (K_T(t) + \frac{K_T(t)}{P_c(t)})dt}}{F_i(0)} - e^{\int_0^t K_T(t)dt}$, are the step response functions to this input. As a sensibility check, Equation 32 shows that if there were

no recovery, that is, if $B(t,t)I(0) = 1$, the infections would grow exponentially until the entire population was infected, an intuitive and reasonable result. This also suggests that, even with a finite recovery period, everyone in the initially affected population, $S(0)$, could eventually become infected.

In a final simplification of the solution, as an approximation, if we assume that both $K_T(t)$ and $P_c(t)$ in Equations 25 through 27 are constant for a period, we arrive at simplified expressions for $N(t)$, $I(t)$, and $R(t)$,

$$N(t) = N(0)e^{-F_i(0)P_c(e^{-\frac{K_T}{P_c}t}-1)} \tag{35}$$

$$I(t) = I(0)e^{-F_i(0)P_c\left(e^{-\frac{K_T}{P_c}t}-1\right)-\frac{K_T}{P_c}t} \tag{36}$$

$$R(t) = (N(0) - I(0)e^{-\frac{K_T}{P_c}t})e^{-F_i(0)P_c(e^{-\frac{K_T}{P_c}t}-1)} \tag{37}$$

Expressions describing an epidemic

Beyond sensibility checks, the availability of a closed form opens a pathway to the derivation of expressions useful in epidemic description and management. These, too, can be easily compared to real world behavior. We illustrate several of these here using the simplifying assumption that K_T and P_c are constants and that $I(0) = N(0) = 1 = F_i(0)$. These simplifying assumptions allow the nature of the expressions to be more easily seen and understood.

Final Size

We first use Equation 35 to find an expression for the final size, $N(\infty)$ as $t \to \infty$,

$$N(\infty) = e^{F_i(0)P_c}. \tag{38}$$

We can see, as suggested by the Step Response form of the solution, that if P_c is large enough, it is possible for $N(\infty)$ to equal $S(0)$.

The time it would take for $N(\infty) = S(0)$ is,

$$t = -\frac{P_c}{K_T} ln(1 - \frac{\ln(S(0))}{F_i(0)P_c}) \tag{39}$$

and the criteria that must be true for the entire population to become infected is,

$$F_i(0)P_c > \ln(S(0)). \tag{40}$$

Equations 38 through 40 enable us to estimate the level of the social interaction that will eventually infect the total population and the time in which this will occur if the social interaction level does not change. To the degree that our simplifying assumptions are valid, we see that the existence of herd immunity is not an inherent property of the Kermack and McKendrick model.

Basic and Effective Reproduction Number, R_0 and R_{Eff}

If we divide $\psi(t)$ into K_T, we find an expression for the Effective Reproduction Number (R_{Eff}):

$$R_{Eff} = \frac{1}{1-F_i(0)e^{-\frac{K_T}{P_c}t}+\frac{1}{P_c}}. \quad (41)$$

A function of both the disease and the behavior of the population, the value of R_{Eff} marks two key epidemic points. First, when $R_{Eff} = 1$, the peak in the number of new infections occurs and the epidemic begins to decline. Second, when $t = 0$, $R_{Eff} = P_c = R_0$; where R_0 is the Basic Reproduction Number.

Time to Peak New Infections and Peak Size

By setting $R_{Eff} = 1$ in Equation 41, we obtain the following expression for the time when the decline in new cases, $\frac{dN(t)}{dt}$, begins:

$$t_{decline} = \frac{P_c \ln(F_i(0)P_c)}{K_T}. \quad (42)$$

Likewise, if we differentiate both sides of Equation 35 twice, we find an expression for the time when $\frac{dN(t)}{dt}$ will be maximal,

$$t_{Peak} = \frac{P_c \ln(F_i(0)P_c)}{K_T}, \quad (43)$$

where t_{Peak} = the time to the peak of new infections. As it should, the peak in new cases coincides with the start of the decline of infections. In addition to sensibility, this illustrates that equations derived from different portions of the closed form solution are consistent.

Equation 43 demonstrates the relationship between the strength of social intervention measures, P_c, and the time to the peak of new infections. When social interventions are stronger (smaller P_c), the time to the peak will always be shorter.

We note here that this relationship between the level of social interaction and the movement of the peak projected by the KMES is the opposite of the projection of this relationship in the SIR models. In the spirit of sensibility and consistency, we highlight this qualitative difference between the projections of the KMES and the SIR models because, as we show later, the data from the Covid-19 pandemic supports the KMES projection.

We can also use Equation 43 and Equation 36 to find the peak value of the infections,

$$I(t)_{Peak} = \frac{I(0)e^{(F_i(0)P_c-1)}}{F_i(0)P_c}. \quad (44)$$

During an epidemic, Equation 44 can be used to estimate the potential level of hospitalizations that may occur by estimating the fraction of infections that result in hospitalizations and then applying it to the right-hand size of the equation.

Section 2: Veracity of the solution using pandemic data

In this section, we first estimate $K_T(t)$ and $P_c(t)$ using early Covid-19 epidemic data. Armed with these estimates, we then project the average viral load in individuals with Covid-19 and the progression of cases in six different countries,

Estimation of $K_T(t)$

With no other a priori information, we continue to assume that, based on where it arises in the model, $K_T(t)$ is a parameter associated with the disease, possibly constant for time intervals in which the infectious agent does not vary. We follow this assumption to its logical conclusion using the data to guide us.

We begin the analysis with a further refinement of the definition of $P_c(t)$. As previously defined, $P_c(t)$ is a function of the population's behavior and is the average number of infectious contacts a member of subpopulation *N*(t) has across the entire population. If we also assume that, during the initial stages of an epidemic, $P_c(t)$ is a function of population density, and that people's infectious mobility extends over an average effective area per unit of time, we can then write an expression for $P_{cr}(t)$:

$$P_{cr}(\mathrm{t}) = \frac{A_{1r}(t)N_p}{A_p} = contact\ rate, \tag{45}$$

where N_p is the entire population of the region with the infection, A_p is the area of the region, $\frac{N_p}{A_p}$ is the population density, and $A_{1r}(t)$ is the area an individual infectiously inhabits per unit time.

Analogous to the way we defined $P_c(t)$ using $P_{cr}(t)$, we now define a quantity, $A_1(t)$, in terms of $A_{1r}(t)$:

$$A_1(t) = \lim_{\Delta t \to 0} \int_t^{t+\Delta t} A_{1r}(t)dt, \tag{46}$$

where $A_1(t)$ is the effective area infectiously inhabited by an individual. In specifying the area, we make an assumption similar to the assumption that we made for $P_c(t)$ in Section 1; that is, the area that a person traverses can change, but we assume that if a change in area alters the ratio $\frac{P_{cni}(t)}{P_c(t)}$, it does so slowly.

We call $A_1(t)$ the "effective area" because the population is typically only physically present within ~1% of the land within a country or region (Ritchie and Roser 2019). If we take this into account, then, $\frac{A_1(t)}{100} = Area\ actually\ traversed\ by\ a\ person.$

We can now write a new expression for $\frac{K_T(t)}{P_c(t)}$:

$$\frac{K_T(t)}{P_c(t)} = \frac{K_T(t)A_p}{A_1(t)N_p}. \tag{47}$$

By substituting Equation 47 into Equation 25, $N(t) = N(0)e^{F_i(0)\int_0^t K_T(t)e^{-\int_0^t \frac{K_T(t)}{P_c(t)}dt}dt}$, assuming that both $N(0)$ and $F_i(0)$ are equal to 1, and both $K_T(t)$ and $P_c(t)$ are constants in the initial stages of the epidemic, we can derive the expression:

$$F(N(t) = \frac{A_1 N_p}{A} \ln\left(1 + \frac{\ln(N(t))}{-\frac{A_1 N_p}{A}}\right) = -K_T t, \tag{48}$$

where we see that if K_T is a constant, then Equation 48 predicts that $F\big(N(t)\big)$ is a linear function of time.

Table 1. Initial COVID-19 pandemic data and population densities for various countries ((Roser et al 2021), case and date data; (Worldometers 2021, population density data)

	Date first case reported	Calculation date	Days between the first case reported and the calculation date	Cases on calculation date, N(t)	Population density (people/km^2)
South Korea	22 Jan	21 Feb	30	204	527
USA	22 Jan	19 Mar	57	13,663	36
Sweden	1 Feb	7 Mar	35	179	25
Italy	31 Jan	24 Feb	24	229	206
Spain	1 Feb	13 Mar	41	5,232	94
New Zealand	28 Feb	19 Mar	20	28	18

All dates are in 2020.

Excepting A_1, all the quantities in Equation 48 can be found for each country in the time before containment measures were enacted. Therefore, we can use equation 48 to assess whether K_T can be reasonably assumed to be constant. Using the values for population density, $N(t)$, and the days between the first case reported and the calculation date found in Table 1 in Equation 48, through a process of iteration, we then determined that the best value for A_1 to create the straight line plotted in Figure 1 was 0.48 km^2. Since we defined A_1 as the effective area, the actual area is 0.0048 km^2, a plausible value.

Fig.1

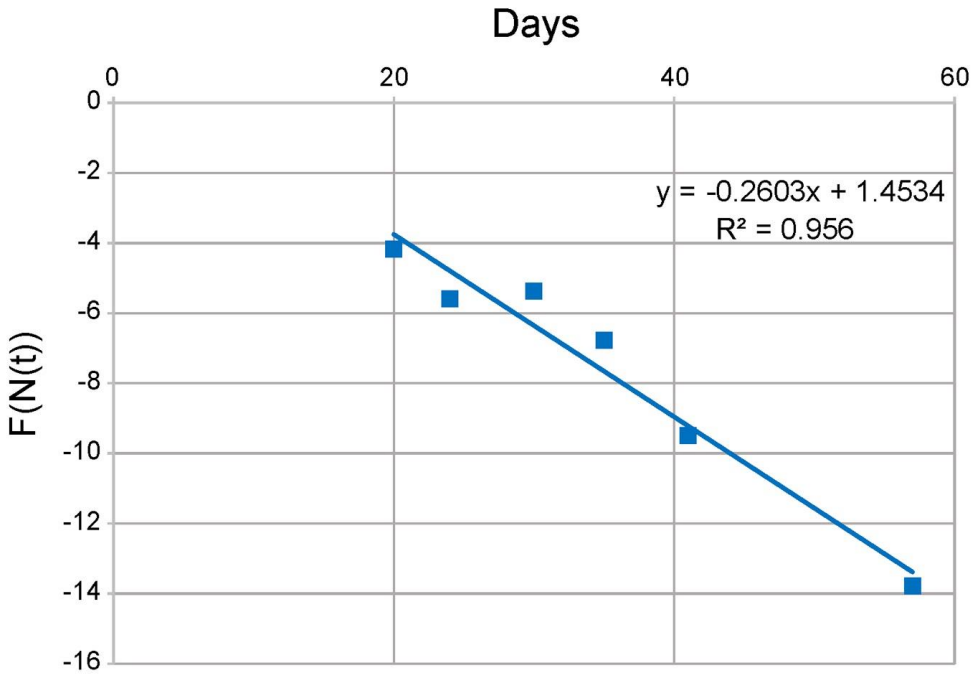

Figure 1. **Verification that K_T is the same for all countries**. The data from Table 1 is plotted using Equation 48 and $A_1 = 0.48\ km^2$. Each data point corresponds to a different country. The value of K_T is the negative of the slope of the line, and K_T is closely approximated everywhere by $K_T \approx 0.26$

As noted in the figure, the line has an $R^2 = 0.956$ as a fit to the data points and the slope of this line is 0.26, the value of K_T. We take the result of this analysis as strong support for the plausibility that, in the initial stages of the pandemic, K_T was a constant across all the sampled countries and is, therefore, appropriately taken to be a parameter of the disease.

Viral Load

We now further support our argument that $K_T(t)$ is a parameter of the disease by demonstrating that the viral load is parameterized solely by $K_T(t)$. We start with the observation

that the step response structure of the KMES suggests that it should also contain an expression for the viral load of the disease.

Equation 29 provides a convenient starting point because it describes the evolution of the infectiousness of the initially infected population. If, in this equation, we continue with the assumption that $K_T(t)$ is a constant; and we set $P_c = I(0) = 1$ (i.e., there was only one initial infection and this infected person contacted, on average, only one person during the epidemic), we then obtain an expression for the infectiousness of the initially infected person,

$$B(t,t) = e^{-(e^{-K_T t}-1)-2K_T t} \tag{49}$$

We know that, as explained in our third thought experiment, infectiousness does not equate to the actual viral load. Rather, it is a measure of the ability to infect and is dependent on the portion of contacts that remain infectable as well as the viral load. Therefore, since the available number of infectable people in P_c is equal to R_{Eff}, we must divide $B(t,t)$ by R_{Eff} (divide Equation 49 by Equation 41) to extract the viral load from the infectiousness. This operation yields (for $P_c = 1$),

$$Viral\ Load = e^{-(e^{-K_T t}-1)-2K_T t}(2 - e^{-K_T t}), \tag{50}$$

and when we then set $K_T = 0.26$ in Equation 50, we obtain Figure 2. Of course, we allow time to be negative in both Equation 50 and Figure 2 at the beginning of the infection because the initially infectious person did not become infected at $t = 0$.

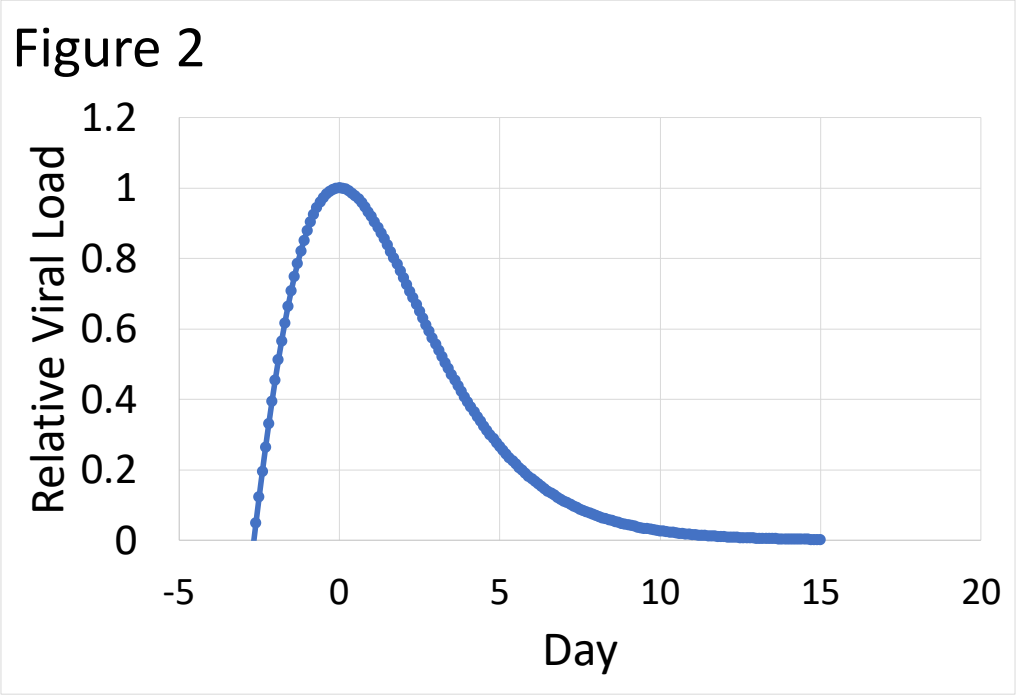

Figure 2. Representation of the normalized viral load of an infected person in the Covid 19 pandemic. The plot was generated using the value $K_T = 0.26$ in Equation 50

As we can see, the plot in Figure 2 has the expected characteristics of a normalized viral load. Rising quickly, it reaches a maximum of 1, and then declines to zero at a slower, exponential pace. To gauge whether the curve in Figure 2, and therefore, Equation 50, truly and adequately represent the normalized viral load, we compared some of its characteristics with those of average viral loads estimated from direct measurements of individual Covid-19 patients.

We find that the curve in Figure 2 has the same overall shape and dynamic change in load from the peak to 15 days later as data measured by Challenger et al (2021) and Jones et al (2022). In these references, using Covid-19 patient data, Challenger et al (2021) found that the base 10 exponential decline rate of the viral load was -0.22 with a credible interval between -0.26

and -0.17 whereas Jones et al (2022) found a credible interval of the base 10 exponential decline of -0.17 to -0.16. A least squares base 10 exponential curve fit to the plot in Figure 2 between day 0 and day 15 has a rate of decline of -0.19 with an R^2 value of 0.99. This result is an indication of the veracity of the KMES and further suggests that K_T is, indeed, a parameter of the disease.

Using the Google Residential Mobility Measure data to Project Country Data

If we assume that both K_T and P_c are at least piece-wise constant for periods of time, we can differentiate both sides of Equation 35, divide the result by $N(t)$, rearrange the terms, and then take the natural log of both sides to obtain the following useful expression,

$$RCO = ln\left(\frac{\frac{dN(t)}{dt}}{N(t)}\right) = \ln(F_i(0)K_T) - \frac{K_T}{P_c}t \qquad (51)$$

We label this the "Rate of Change Operator" (RCO) because it is a measure of the rate of change of $N(t)$, per person within $N(t)$. Given an estimate for K_T, the RCO is particularly useful for projecting current epidemic conditions because only the readily available contemporaneous values of $N(t)$ and $\frac{dN(t)}{dt}$ are required to estimate the current values of both P_c and $F_i(0)$.

We begin the development of epidemic projections by first applying Equation 51 to data (Roser, et al. 2021) from six different countries during the initial stages of the Covid-19 pandemic to create the curves in Figure 3. As can be seen in that figure, there is a period both before and shortly after the date of the imposition of containment actions in the six countries

Figure 3 (A-F)

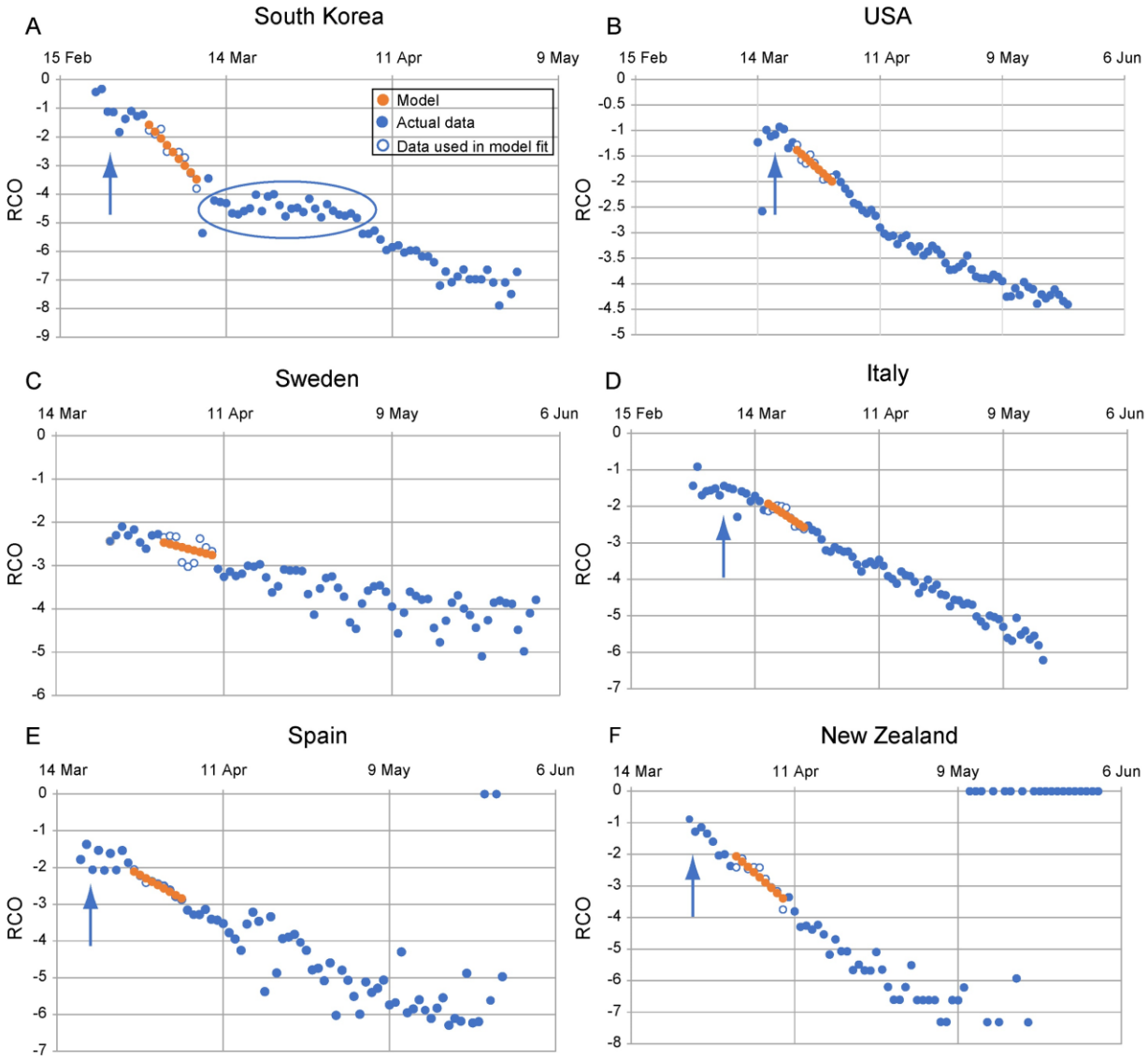

Figure 3. Rate of change operator (RCO) curves for COVID-19 cases in various countries. An epidemic can be described by a piecewise linear model using the RCO (Equation 52). A short segment of orange dots in each graph is a linear fit to the corresponding points (blue/white circles) in the observed data. The slopes of these dotted-line segments are the values of $\frac{K_T}{P_c}$ which are tabulated in Table1. In some countries, RCO curves changed markedly soon after the date containment measures were implemented (arrows): **A)** South Korea, February 21; (the oval highlights a departure of the observed data from the RCO slope, indicating failures in, or relaxations of, social distancing); **B)** USA, March 16; **C)** Sweden did not implement any specific containment measures, so the model calibration was begun on April 1, the date when the slope of the RCO curve first became steady. **D)** Italy, March 8; **E)** Spain, March 14; **F)** New Zealand, March 25. All dates are in 2020.

when these RCO curves became straight lines; an indication that it is reasonable to assume that K_T and P_c were approximately constant during this period.

We subsequently determined the value of $\frac{K_T}{P_c}$ by fitting Equation 51 to short, nine data point portions early in the straight segments of the RCO time series. We assumed that this fitted value was valid for the first time point in the series. We then calibrated the values for P_c to Google's Residential Mobility Measure (Google 2023) for each country on that first date using the expression:

$$P_{cal} = \frac{-K_T(t)}{Slope(1-\frac{G_{R0}}{100})}, \quad (52)$$

where $\frac{K_T}{P_c} = Slope$ and G_{R0} is the value of the Google Residential Mobility Measure on the same first date. The P_{cal} values and dates used for each country are listed in Table 2.

Having calibrated P_c to the Google Residential Mobility value on a single date, we then used the sequence of Google Residential Mobility data following that date to find the subsequent daily values of $P_c(t)$ by multiplying P_{cal} by $(1-\frac{G_R}{100})$ (where G_R is the Google Residential Mobility Measure for that date). Using the value of $K_T(t)$ from Figure 4 and these daily values of $P_c(t)$, we then employed Equation 25 to project the course of daily total cases (Figure 4) for the six countries. These predictions matched the actual time series of the daily <u>total</u> cases with an $R^2 > 0.85$ in each of the six countries for the 60 days following the date P_{cal} was calculated.

We also used the derivative of Equation 25 to plot the predicted time series of the daily <u>new</u> cases in Figure 5 for the six countries for the same 60 days. These predictions have an R^2

range of 0.01 (Sweden) to 0.94 (New Zealand); and as seen in the figure, the predicted peak of new cases was close to the observed peak for all countries.

We emphasize that the predictions in Figures 4 and 5 are *not* fits to the full length of the data shown. Rather, one constant, P_{cal}, for the indicated dates was estimated using only a short, linear portion of the epidemic data starting between 7 to 14 days after the imposition of containment measures. P_{cal}, the prior estimate of K_T and the Google Residential Mobility Measure for each subsequent day were then used to project the rest of the data.

Table 2. Parameters used to model total cases and new daily cases of infection for different countries.

	$\frac{K_T}{P_c}$	P_{cal}	Date range for RCO fit
South Korea	0.22	1.35	February 29–March 8
USA	0.076	4.10	March 23–March 31
Sweden	0.036	8.04	April 1–April 9
Italy	0.080	4.55	March 17–March 25
Spain	0.099	3.76	March 26–April 3
New Zealand	0.12	2.65	March 27–April 4

Parameters from linear fit of rate of change operator (RCO) data in Figure 1. $\frac{K_T}{P_c}$ (slope); P_{cal} was calculated using Equation A: $P_{cal} = \frac{-K_T(t)}{Slope(1-\frac{G_{R0}}{100})}$. The value for G_{R0} was the value of the Google Residential Mobility Measure for that country on the first date in the listed date ranges. All dates are in 2020.

Fig. 4 (A-F)

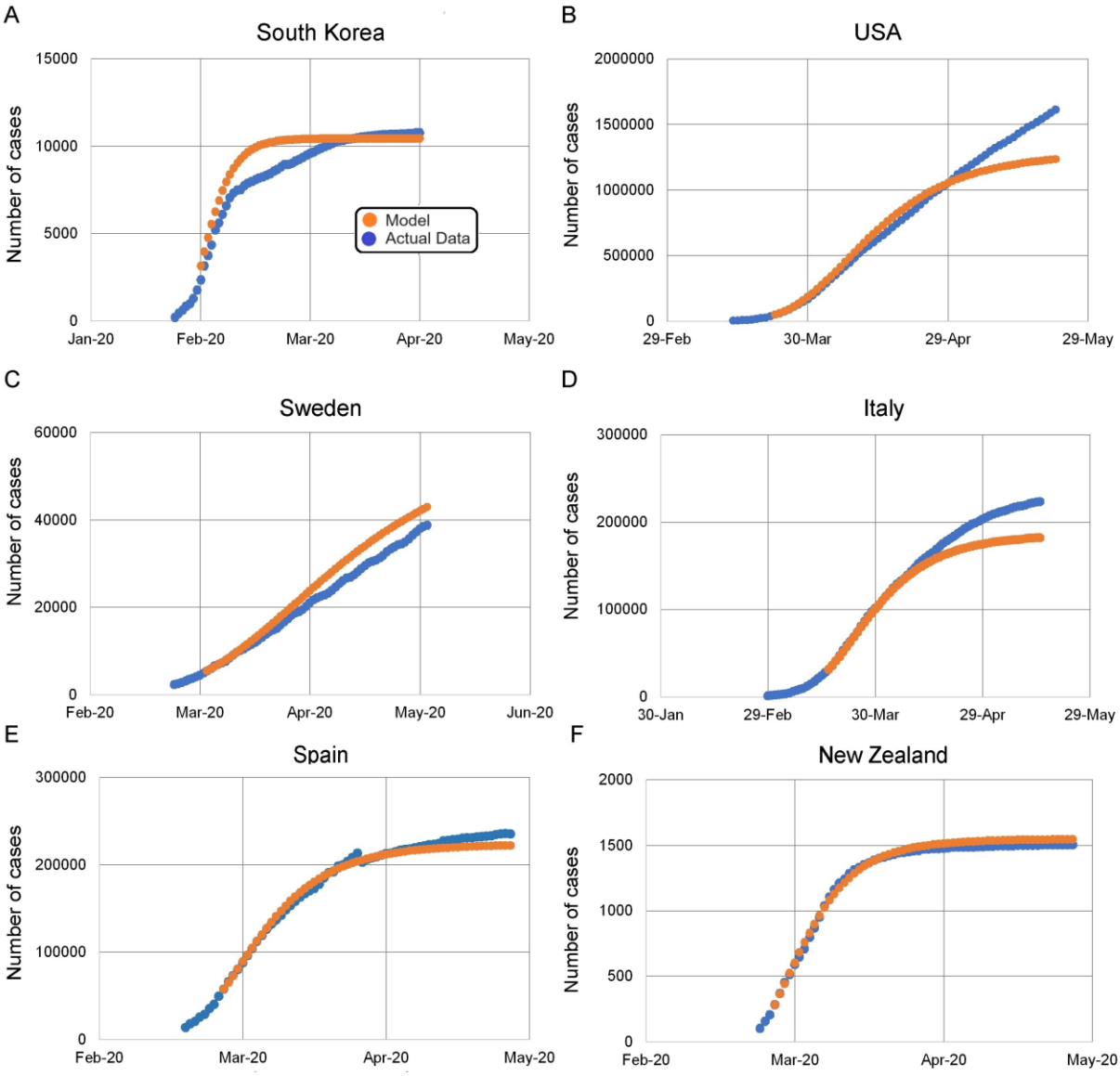

Figure 4. Complete KMES model predictions for daily total case counts. A) South Korea; **B)** USA; **C)** Sweden; **D)** Italy; **E)** Spain; and **F)** New Zealand. Dots are daily data points observed from (white-center and all blue) or calculated (orange) for each country. The KMES model was calibrated using data from the date ranges listed in Table 2. $R^2 > 0.85$ for the model fit for all countries for the 60 days after the P_{cal} was calculated: South Korea, March1-April 29; USA, March 24-May 22; Italy, March 18–May 16; Spain, March 27-Maz 25; New Zealand, March 27-May 25. Sweden April 2- May 31. The deviation of the model from the data in the USA, panel (**B**), after April is elucidated in Supplement 2. All dates are in 2020.

Fig.5 (A-F)

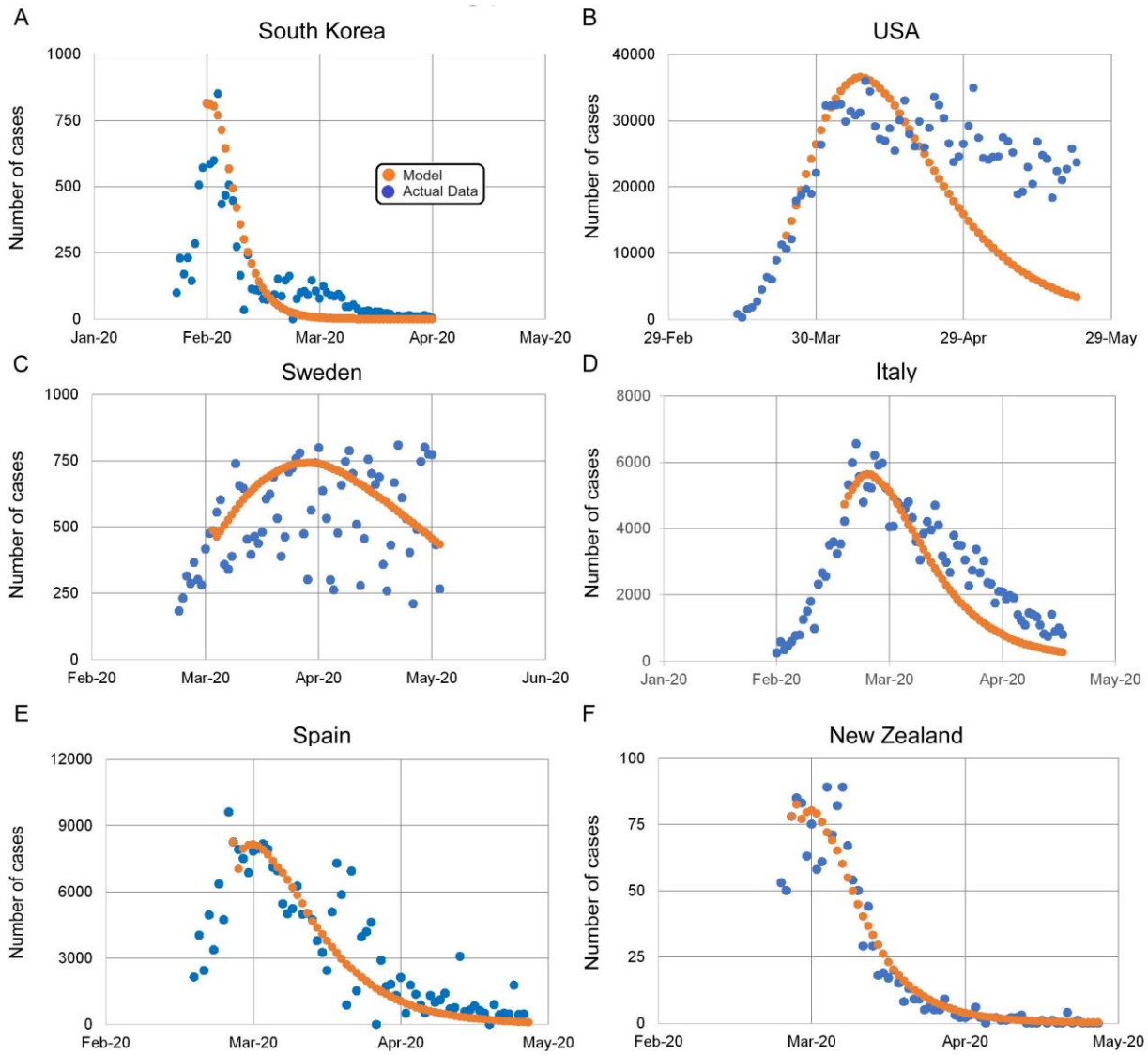

Figure 5. Complete KMES model predictions for number of new daily cases. A) South Korea, $R^2 = 0.87$; **B)** USA, $R^2 = 0.31$; **C)** Sweden, $R^2 = 0.01$; **D)** Italy, $R^2 = 0.88$; **E)** Spain, $R^2 = 0.82$; and **F)** New Zealand, $R^2 = 0.94$. The orange dotted line is the model in all panels. The blue dots are the daily observations from each country. The. R^2 values are between the model and the data, across countries for the 45 days after containment measures were instituted.

Section 3: Managing an Epidemic

An important decision to be made during an epidemic is whether to strengthen or loosen restrictions on social interactions. To illustrate how the strengthening of restrictions can affect the epidemic outcome, in Figure 6 we present a plot of the total cases and new cases per day for four countries in two pairs. We created the figure by matching countries with similar populations densities and then assuming this meant their baseline social interaction levels were similar. We selected these specific countries, because, in a presumably unintentional natural experiment, the paired countries imposed very different social restrictions at the outset of the Covid-19 pandemic, and as can be seen in the figure, their outcomes were very different.

Fig.6 (A-D)

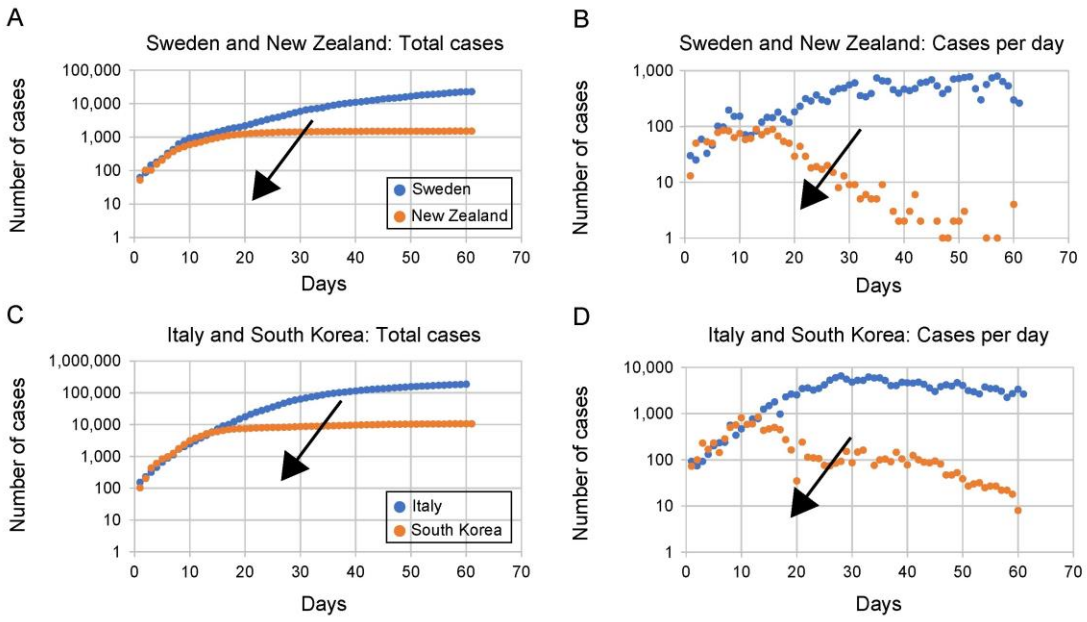

Figure 6. Total cases and new cases per day for countries with comparable population densities, which employed different levels of social containment.

In the countries which imposed strict policies (New Zealand and South Korea) the total cases leveled off sooner and the new cases per day peaked earlier than in their matching countries, Sweden and Spain which imposed less stringent restrictions. This is an intuitive result, the sort of thing that a veracious epidemic model should project.

Of course, it is straightforward to look back in time at data and prescribe a better course of action. Since we do not have this luxury at the outset of a pandemic, we need a model that accurately projects trends and provides decision support. To this end, we can compare how the KMES and SIR approximations project the way new cases will trend as social interactions change.

In Figure 7, we plot simulations of both the SIR approximation and the KMES. We used Equation 35 to create the KMES simulation and an Euler approximation to solve the simple SIR model found in Brauer (2008)..

$$\frac{dS(t)}{dt} = -\frac{\beta I(t)S(t)}{N_p}, \tag{53}$$

$$\frac{dI(t)}{dt} = \frac{\beta I(t)S(t)}{N_p} - \gamma I(t), \tag{54}$$

$$\frac{dR(t)}{dt} = \gamma I(t), \text{ and} \tag{55}$$

$$N_p = S(t) + I(t) + R(t), \tag{56}$$

where β and γ are constants

Fig.7 (A-D)

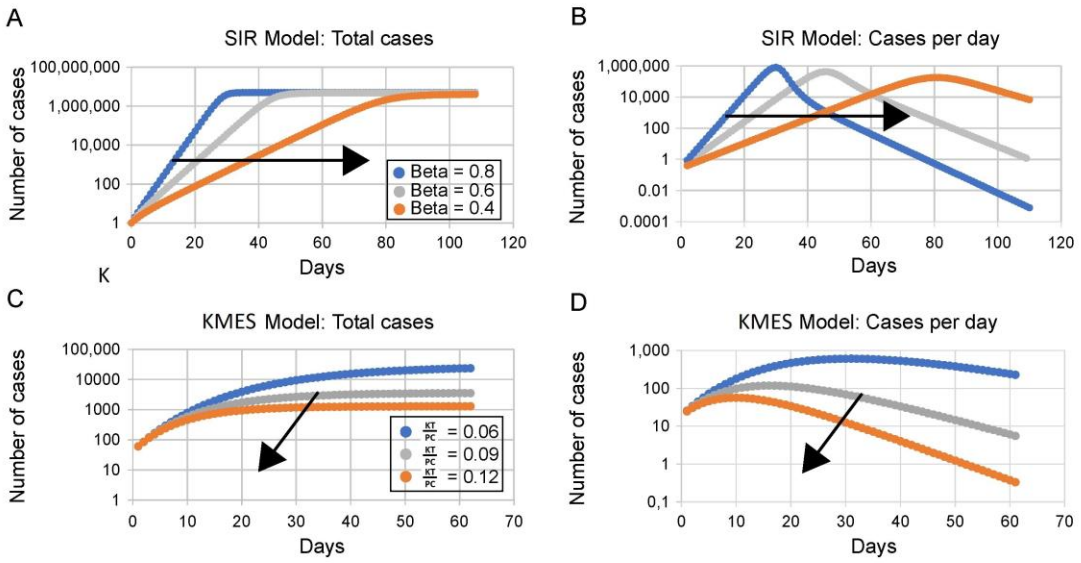

Figure 7. SIR and KMES simulations with varying levels of social restrictions. The arrows point in the direction the curves trend as the social restrictions are increased. The value of $\gamma = 0.2$ in the upper two panels and $K_T = 0.26$ in the lower two panels.

As is easily seen in Plots 6A and B, more social restrictions in the SIR approximation (lower β) result in both the plateau of total cases and the peak in new cases occurring later, projections which do not match the data from the countries in Figure 6. This does, however, illustrate the phenomenon known as "Flatten the Curve" (Dilaurio, F., et al, 2011) and the analytical results for the SIR model in (Kröger and Schlickeiser, 2020).

In contrast, as seen in the lower panels in the figure, the KMES projects that a peak in daily new infections will occur earlier (Plot D in Figure 7; supported by Equations 42 and 43) and that total infections will plateau sooner (Plot C in Figure 7) with less social interaction (lower values of $P_c(t)$). These trend projections are, in fact, intuitive, and match well the trends

of the actual case data in Figure 6. This supports the veracity of the KMES and contradicts the projections of SIR models.

Diagnosing the status of an Epidemic

Motivated by the observation that the existing, accepted model of epidemics, the SIR model fails to project even the qualitative features of the observed, paired country data, in the remainder of this section we demonstrate how to use the analytical expressions developed from the KMES in Section 1 to characterize an ongoing epidemic. Then, based on this characterization, we suggest how policy recommendations for the public with the aim of ending an epidemic could be made.

We first demonstrate the ability of the KMES to project future cases using the United States data from the Covid-19 pandemic. We make this projection by first calculating the value of the RCO on a given day and the seven previous days. We then fit Equation 51 to those eight known values to find their intercept, $\ln(F_i(0)K_T)$, and slope, $\frac{K_T}{P_c}$. We assumed that these values were constant for those prior eight days and remained constant for the following 21 days, a total of 29 days. Using these in Equation 35 with the time set to 21 days, along with the value of the total cases on the chosen day, we projected the total cases 21 days into the future.

Figure 8 is a plot of that projection overlaid onto a plot of the actual total case data for 554 days following April 30, 2020. As seen in the figure, the KMES was relatively consistent in accurately projecting the cases 21 days in advance. The projected data points have a Mean Absolute Percentage Error of 4.1% over the entire period when compared to the actual values.

Figure 8 demonstrates the projection power of the KMES; however, a projection alone is not adequate for addressing a paramount goal of public health management: recognizing and avoiding outbreaks. For detecting emerging outbreaks, we must use a measure which reflects the underlying dynamics, such as the R_{Eff}. Fortunately, if we have an estimate of K_T, we can always determine the daily value of the R_{Eff} by calculating the contemporaneous RCO and using the result in a restatement of Equation 41,

$$R_{Eff} = \frac{1}{1-\frac{e^{RCO(t)}}{K_T}+\frac{1}{P_C}}. \tag{57}$$

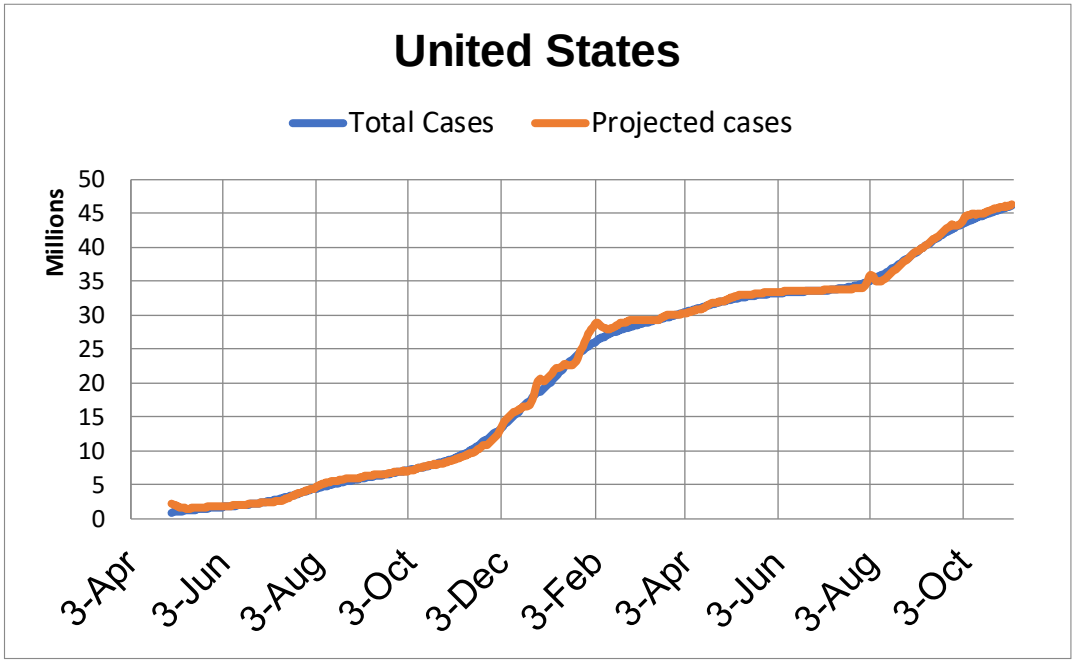

Figure 8. Projection of cases in the United States from April 25, 2020 to November 4, 2021. The Orange line is the projection of cases 21 days in the future from the point of each actual data point.

Of course, we must also first use the technique demonstrated above to evaluate $\frac{K_T}{P_c}$ to then find the value of $\frac{1}{P_c}$ for use in Equation 57.

Figure 9 depicts the application of Equation 57 to the US Covid-19 data (Roser et al, 2021) for new daily cases over the same time frame as was used in Figure 8. The blue area represents the new daily cases, and the orange strip denotes the period when the 7-day average R_{Eff} (computed over the prior 7 days) was greater than 1. The start of each orange section marks the beginning of an outbreak; and at the end of each orange section, (where $R_{Eff} < 1$), we find the peak in the daily new cases, as might be expected.

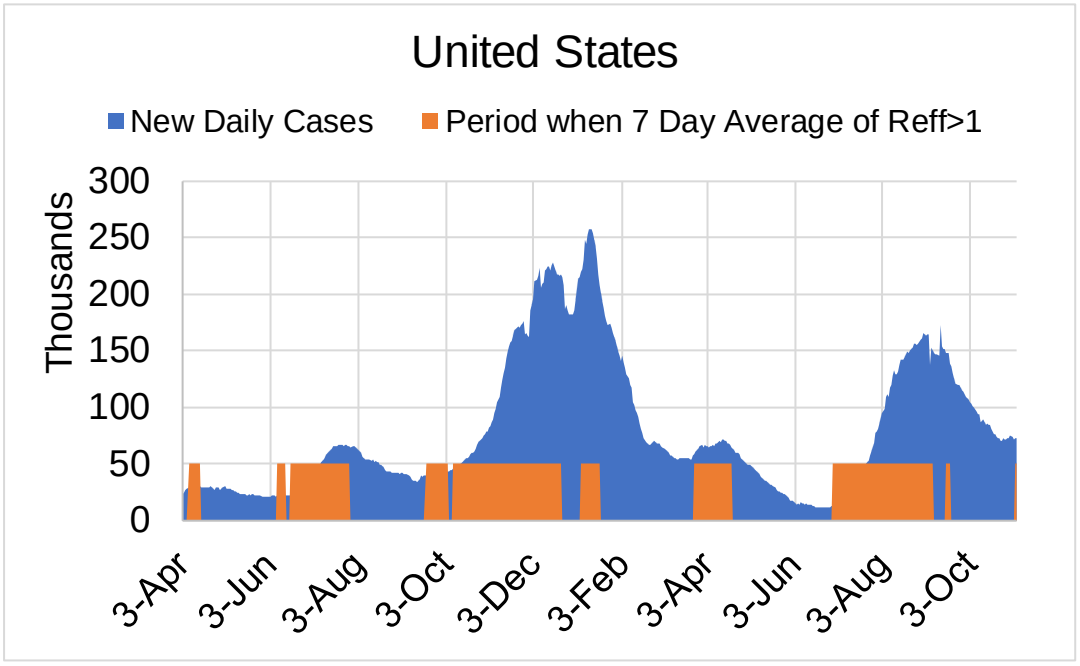

Figure 9. Periods when the 7-day average $R_{Eff} > 1$. The Orange areas indicate the periods when the R_{Eff} averaged above 1 for the prior 7 days.

Controlling the Epidemic

If the calculation of R_{Eff} identifies an outbreak, social policies should immediately be modified to blunt the impact. Here we demonstrate how expressions based on the KMES can be used both to set out a program for gaining control of the emerging outbreak and then to determine how those control measures might be adjusted to manage the epidemic in a fashion consistent with social and political realities.

We start by defining the acceleration of an epidemic as the derivative of $\frac{dN(t)}{dt}$. This can be derived by differentiating Equation 35 twice:

$$\frac{d^2N(t)}{d^2t} = \left(K_T F_i(0) e^{-\frac{K_T}{P_c}t} - \frac{K_T}{P_c}\right)\frac{dN(t)}{dt} = K_T\left(\frac{I(t)}{N(t)} - \frac{1}{P_c}\right)\frac{dN(t)}{dt} = \left(e^{RCO(t)} - \frac{K_T}{P_c}\right)\frac{dN(t)}{dt} = K_T\frac{dI(t)}{dt}. \quad (58)$$

Equation 58, with its four equivalent expressions can be used to quickly determine whether the control measures in place, represented by P_c, are sufficiently effective. When the term, $e^{RCO(t)} - \frac{K_T}{P_c}$, in the third equality is positive, then the control measures are not strong enough; and conversely, when this term is negative, the epidemic is being brought under control. We note that this latter condition is coincident with $R_{Eff} < 1$.

The maximum value of P_c that will begin to bring down the new cases per day is the quantity upon which management strategies pivot. If we set the left-hand side of Equation 58 to zero, use the third expression from the left in Equation 58 and solve for P_c, we arrive at a defining relationship for this critical objective of epidemic management:

$$P_c < K_T e^{-RCO(t)}. \tag{59}$$

Equation 59 succinctly states that P_c must be managed to stay below $K_T e^{-RCO(t)}$ to ensure that the acceleration is negative and therefore, slow the epidemic. Since the $RCO(t)$ can be computed every day and K_T can be estimated using the technique illustrated in Section 2, the maximum level of infectable social contact allowable (P_c in Equation 59) to start or continue decreasing the number of new cases per day can always be calculated. (As a side comment, and as explained in Supplement 3.1, if the slope of the RCO curve is determined from the graphical analysis to be greater than zero, then an outbreak has occurred and immediate reductions in social interactions are needed.)

If the situation warrants, we can determine the time needed to reach a desired reduction in $\frac{dN(t)}{dt}$, at a future time, $t + t_{target}$ for a given level of social interaction. If we define the fractional reduction in cases we desire as D_{tf},

$$D_{tf} = \frac{\frac{dN\left(t+t_{target}\right)}{dt}}{\frac{dN(t)}{dt}} = \frac{New\ Case\ Target\ Rate}{Current\ New\ Case\ Rate}, \tag{60}$$

then, using the derivative of Equation 35, we arrive at the following expression:

$$D_{tf} = e^{-P_c\left(e^{-\frac{K_T}{P_c}(t+t_{target})} - e^{-\frac{K_T}{P_c}(t)}\right)} e^{-\frac{K_T}{P_c}t_{\text{target}}}. \tag{61}$$

If $t \gg t_{target}$, then $e^{-\frac{K_T}{P_c}(t+t_{target})} - e^{-\frac{K_T}{P_c}(t)} \approx 0$ and we obtain the following equation from the remaining terms:

$$t_{target} = -\frac{P_c \ln (D_{tf})}{K_T}. \quad (62)$$

Equation 62 quantitates the number of days, t_{target}, that a level of social containment, P_c, must be maintained to reach a desired reduction of the current daily cases.

As an example, in the case of the United States, based on the data shown in Figure 9, a very large outbreak started in the last days of September and early October 2020. On October 10, 2020, there were 58.082 new cases and the outbreak peaked January 8, 2021, 90 days later with 283,204 recorded cases. Had the US implemented a social program to reduce the number of average infectious contacts (P_c) to 10 people for those same 90 days, instead of an outbreak and a peak, equation 62 projects that the number of new cases on January 8, 2021 would have been approximately 5800, a 98% reduction from the actual value. In Supplement 2, we present further examples and additional insights utilizing the data in several additional countries.

Discussion

In response to Diekmann's call for action, the "wisdom" we believe we have found in the Kermack and McKendrick integro-differential equations appears to be substantial. Foremost, we suggest that the KMES obviates the need for any approximation to these same equations. Rather than use an approximation, such as the SIR special case, we can instead use the KMES itself to predict the dynamics of an epidemic, to determine whether the societal controls in place are adequately managing the epidemic, and to develop quantitative measures for guiding the behavior of the populace.

It is reassuring that the KMES has an intuitive form, as exemplified by the systems view encapsulated in Equation 32:

$$I(t) = e^{\int_0^t K_T(t)dt} B(t,t) I(0) \qquad (32)$$

This equation states that the input of infections, $B(t,t)I(0)$, is transformed into the time varying output of infectiousness, $I(t)$, through an exponential step response function, $e^{\int_0^t K_T(t)dt}$. Our analysis has led us to affirm this obvious-in-retrospect, practical mathematical characterization of epidemic dynamics.

The KMES also fulfills other expectations. As a first example, we recognize Equations 25 and 35 as Gompertz equations. This form is supported by Onishi et al (2021) who demonstrated that the Covid-19 epidemic time course in many countries was well fit by a Gompertz model. These authors do not offer a basic principles argument as to why this is so, but they demonstrate a strong correlation to this aspect of our model structure. Additionally, using the independently measured population mobility in the Google data, we found that the KMES accurately projects phenomena which arose in the Covid epidemic. This contrasts with the weak correlations of the SIR construct to mobile phone mobility data found by prior authors (Wesolowski 2015).

With the availability of an analytical solution, previously unknown, pragmatic expressions of key epidemiological relationships were found for the following: Time course of the epidemic size; Final epidemic size; Time to peak infections; Effective Reproduction number; Viral load; as well as expressions for targets for reducing the size of an epidemic along a planned

path. The KMES also enabled us to illustrate that phenomena predicted using the SIR approximation, herd immunity and "flatten the curve", are not, in fact, properties of the Kermack and McKendrick integro-differential equations. Therefore, we suggest that the analytical expressions derived from the KMES should become the first elements in a new toolbox for public health officials.

Conveniently and convincingly, these expressions agree with intuition and behave sensibly. For instance, the model expression for Time to the peak in new cases, in Equations 42 or 43, passes smoothly through the epidemic maximum as the value of R_{Eff} passes through one as the social interactions are decreased by reducing the value of P_c. This contrasts with the behavior of the expression for the time to the peak derived from SIR models (Kröger and Schlickeiser, 2020; Equation 59 and Figure 5). While we do not doubt that their expressions have been correctly derived from the SIR equations, their expressions do show that, for a given population size and initial value of $I(0)$, the estimated time to the peak in new infections becomes increasingly larger as social interactions are decreased and R_{Eff} approaches the value one. The time to the peak in new infections then suddenly plunges to negative infinity just as R_{Eff} reaches one. This peculiarity mathematically summarizes the claimed phenomena behind the concept of "flattening the curve", but it is unsettling and nonintuitive.

Our expressions for the time to the peak, Equations 42 and 43, have none of this peculiar behavior and, as we've demonstrated using Figure 4 and 5, the form of these equations fit well the data from different countries which imposed very different containment strategies. These equations show that as people interact less frequently (social containment is increased), the peak

number of infections is much lower, and it occurs earlier. The KMES shows that strong containment actions shorten the epidemic, as one would intuit; and as data from several countries clearly demonstrate. This finding is also supported by the data presented in Figure 4 in Harris (2023).

Our expression for the final epidemic size conflicts with an oft derived tenet of epidemiology: that an entire population cannot become infected, the so-called phenomenon of herd immunity. Equations 38 through 40, mathematical expressions for the final size, the time to reach it and the associated contact required, in their mathematical simplicity, give voice to the intuitive conclusion that if the people contact each other infectiously at a high enough level for a long enough time, an epidemic can spread to an entire population and herd immunity is not guaranteed. Epidemiology should be freed from this tautology.

It should not be surprising that a closed form, complete solution to the epidemic equations produces an expression for the viral load. The curve in Figure 2, wholly derived from the Covid-19 data, has the characteristics many investigators have expected a viral load to have (Challenger et al 2022, Jones et al 2021, Diekmann 2022). While Jones and Challenger reached their conclusions through direct measurement of the viral load of thousands of patients, the same form has emerged from the KMES using only the country case data.

Equations 26 and 27 show that both $I(t)$ and $R(t)$ directly depend on both $K_T(t)$, a property of the disease and $P_C(t)$, a function of the population behavior. It is intuitive and obvious that both $I(t)$ and $R(t)$ will depend on properties of the disease, but the form of the KMES demonstrates the equally obvious fact that their values also depend on the behavior of the

population. We explain this dependency in Section 1 and Supplement 1 by showing that $I(t)$ is best interpreted as the total infectiousness within the infected population $N(t)$. As a complementary interpretation, $R(t)$ is best thought of as the degree of recovery from infectiousness within $N(t)$. Therefore, a previously infected individual is simultaneously a part of both the infected and recovered populations with the degree of membership determined by the parameter $\psi(t)$.

As time goes on, the degree of membership inevitably moves infected individuals towards membership in the recovered community, but during this time, the infectiousness of all individuals vary with both their viral load and number of contacts. An increase in social contact causes an increase in infectiousness, which, in turn, decreases the degree to which the person remains in the recovered population and vice versa. Therefore, as an individual's viral load changes, based on time and the disease dynamics, so too, does this individual's ability to infect others change based on their level of social interaction.

This concept of variable membership erodes the utility and fidelity of a compartmental model wherein people move irreversibly from being infected to recovered. Rather, assuming individual immunity exists, the proper construct is that there are only two compartments: 1) not yet infected, $S(t)$; and 2) previously infected, $N(t)$; and only from the latter of these is there no escape.

We recognize that our analysis can be improved by an exploration of population interactions that differ from the ones we assumed. For instance, we made the simplifying

assumption that the ratio $\frac{P_{cni}(t)}{P_c(t)}$ remains constant as P_c changes. This is a reasonable assumption, but an analysis which does not require its use may provide even deeper insights into epidemic behavior and management.

The analysis can also be further improved by using the enormous amount of case data now available. This additional data can improve the estimate of the key parameter, $K_T(t)$, including variations in time (with mutations of the infectious agent) and possibly with local genetic variations in the population affected. This could further elucidate the actions people and governments need to take to achieve the target values of $P_c(t)$.

The KMES provides new logical and analytical tools to quickly and easily characterize the state of an epidemic and provide guidance to public health officials. These tools show, unequivocally, that with stronger initial measures, an epidemic can be stopped more quickly with much less economic damage than predicted by conventional models. Although each disease agent will have its own infectious process, the overall epidemic dynamics can ultimately be controlled by the behavior of the population; and the KMES quantitates the necessary level of that control.

References

Brauer, F. (2008). Compartmental Models in Epidemiology. In: Brauer, F., van den Driessche, P., Wu, J. (eds) Mathematical Epidemiology. Lecture Notes in Mathematics, vol 1945. Springer, Berlin, Heidelberg. https://doi.org/10.1007/978-3-540-78911-6_2

Breda D, Diekmann O, de Graaf W F, Pugliese A, Vermiglio R On the formulation of epidemic models (an appraisal of Kermack and McKendrick). Journal of Biological Dynamics, 2021, 6:sup2, 103-117, DOI: 10.1080/17513758.2012.716454

Campbell C. South Korea's health minister on how his country is beating coronavirus without a lockdown. TIME. https://time.com/5830594/south-korea-covid19-coronavirus/ (2020). Published April 30, 2020. Accessed February 9, 2021.

Challenger JD, Foo CY, Wu Y, Yan AWC, Marjaneh MM, Liew F, Thwaites RS, Okell LC, Cunnington AJ. Modelling upper respiratory viral load dynamics of SARS-CoV-2, BMC Medicine (2022) 20:25 https://doi.org/10.1186/s12916-021-02220-0

Di Lauro F, Berthouze L, Dorey MD, Miller JC, Kiss IZ. The Impact of Contact Structure and Mixing on Control Measures and Disease-Induced Herd Immunity in Epidemic Models: A Mean-Field Model Perspective, Bulletin of Mathematical Biology (2021) 83:117 https://doi.org/10.1007/s11538-021-00947-8

Diekmann O, European Communications in Mathematical and Theoretical Biology 2022 No. 24, pgs 7-9

Diekmann O, De Jong M C M, Metz J A J, A Deterministic Epidemic Model Taking Account of Repeated Contacts between the Same Individuals Journal of Applied Probability, Vol. 35, No. 2. (Jun., 1998), pp. 448-462

Diekmann O, Othmer H G, Planque R, Bootsma, M C. The discrete-time Kermack–McKendrick model: A versatile and computationally attractive framework for modeling epidemics. PNAS 2021 Vol. 118 No. 39 e2106332118. https://doi.org/10.1073/pnas.2106332118

Elassar A, This is where each state is during its phased reopening. CNN. https://edition.cnn.com/interactive/2020/us/states-reopen-coronavirus-trnd. Published May 27, 2020. Accessed February 9, 2021.

Field A, New Zealand isn't just flattening the curve. It's squashing it. The Washington Post. https://www.washingtonpost.com/world/asia_pacific/new-zealand-isnt-just-flattening-the-curve-its-squashing-it/2020/04/07/6cab3a4a-7822-11ea-a311-adb1344719a9_story.html. Published April 7, 2020. Accessed February 9, 2021.

Google community mobility reports. https://www.google.com/covid19/mobility/. Published September 20, 2023. Accessed September 20, 2023.

Harris, JE. Mobility was a Significant Determinant of Reported COVID-19 Incidence During the Omicron Surge in the Most Populous U.S. Counties. BMC Infectious Diseases (2023) 22:691. https://doi.org/10.1186/s12879-022-07666-y

Jones TC, Biele G, Mühlemann B, Veith T, Schneider J, Beheim-Schwarzbach J, Bleicker T, Tesch J, Schmidt ML, Sander LE, Kurth F, Menzel P, Schwarzer R, Zuchowski M, Hofmann J, Krumbholz A, Stein A, Edelmann A, Corman VM, Drosten C. Estimating

infectiousness throughout SARS-CoV-2 infection course, Science 9 July 2021 373, eabi5273, https://doi.org/10.1126/science.abi5273

Kermack WO, McKendrick AG. A contribution to the mathematical theory of epidemics, Proc R Soc Lond A. 1927, 115(772):700–721. https://doi.org/10.1098/rspa.1927.0118

Kröger M, Schlickeiser R. Analytical solution of the SIR-model for the temporal evolution of epidemics. Part A: Time-independent reproduction factor. J Phys A Math Theor. 2020;53:505601

Newman, M E J, Spread of epidemic disease on networks, PHYSICAL REVIEW E **66**, 016128, 2002

Ohnishi A, Namekawa Y, Fukui T. Universality in COVID-19 spread in view of the Gompertz function. Prog. Theor. Exp. Phys. 2020, 12:123J01. https://doi.org/10.1093/ptep/ptaa148

Ritchie H, Roser M. Land use. Our world in data. https://ourworldindata.org/land-use Published September 2019. Accessed February 9, 2021.

Roser M, Ritchie H, Ortiz-Ospina E, et al. Coronavirus pandemic (COVID-19). Our World in Data. https://ourworldindata.org/coronavirus. Published December 2, 2021. Accessed December 2, 2021.

Wesolowski A, Metcalf CJE, Eagle N, Kombich J, Grenfell BT, Bjørnstad ON, Lessler J, Tatemc AJ, Buckee CO Quantifying seasonal population fluxes driving rubella transmission dynamics using mobile phone data. PNAS 2015 Vol. 112 No. 35 11114-11119. www.pnas.org/cgi/doi/10.1073/pnas.1423542112

Worldometers. https://.worldometers.info. Published August 21, 2021. Accessed August 21, 2021

Youssef M, Scoglio C, An individual-based approach to SIR epidemics in contact networks, Journal of Theoretical Biology, Volume 283, Issue 1, 21 August 2011, Pages 136-144, https://doi.org/10.1016/j.jtbi.2011.05.029

Supplement 1 Insights developed from the KMES

As we derived the KMES, we did not stop to detail insights provided by some of the important expressions. In this section, we will provide those insights.

The first expression is the relationship described by the derivative of Equation 32:

$$\frac{d\left(\frac{I(t)}{N(t)}\right)}{dt} = -\frac{K_T(t)I(t)}{P_c(t)N(t)} \tag{23}$$

This seemingly simple expression is, along with Equation 2, a fundamental statement of an infectious epidemic.

If we write out the derivative, $\frac{d\left(\frac{I(t)}{N(t)}\right)}{dt}$, in Equation S1-1, we obtain:

$$\frac{d\left(\frac{I(t)}{N(t)}\right)}{dt} = \frac{d(I(t)}{dt}\frac{1}{N(t)} - \frac{dN(t)}{dt}\frac{I(t)}{N(t)^2} = -\frac{I(t)}{N(t)}\frac{K_{\mathrm{T}}(t)}{P_c(t)} \tag{S1-2}$$

With some rearrangement of the terms, we find the following expression:

$$\frac{d\left(\frac{I(t)}{N(t)}\right)}{dt} = \frac{\frac{dI(t)}{dt} - \frac{dN(t)}{dt}\frac{I(t)}{N(t)}}{N(t)} = \frac{-I(t)\frac{K_{\mathrm{T}}(t)}{P_c(t)}}{N(t)} \tag{S1-3}$$

We highlight equation S1-3, because it brings to light an important insight when we set $t = 0$, and $I(0) = N(0)$. Setting $I(0) = N(0)$ and $t = 0$ in Equation S1-3 and recognizing that $\frac{dN(t)}{dt} - \frac{dI(t)}{dt} = \frac{dR(t)}{dt}$ we obtain the following:

$$\frac{dR(0)}{dt} = I(0)\frac{K_{\mathrm{T}}(0)}{P_c(0)} \tag{S1-4}$$

Since all three quantities on the righthand side are positive, Equation S1-4 provides a possibly startling result: The recovered population begins to grow the instant the epidemic starts!

Furthermore, Equation S1-4 tells us that the infectiousness of the individuals in the population $I(0)$ (and by extension $I(t)$) is not a constant during the time they are infected. This may be obvious because the viral load changes as the infectiousness of a person changes. However, Equation S1-4 handily provides us with the initial rate at which the infectiousness of population $I(0)$ is changing. That rate is $\frac{K_{\mathrm{T}}(0)}{P_c(0)}$.

It is not surprising that disease infectiousness is a function of K_{T} but it is perhaps less obvious that the infectiousness changes directly and inversely to the population behavior, P_{c}. The infectiousness of a person is not just dependent on the viral load, but also and comparably so

on the contacts a person has with other, not-yet-infected people. Semantically, if an infected person never contacts another noninfected person, they are never truly infectious in the sense that they cannot advance the disease. We can describe $R(t)$ in an obverse manner, since $R(t)$ is the reduction in the total infectiousness that has occurred in the population, $N(t)$; and so, it is also a function of the disease transmissibility and population behavior.

We gain further insight into the meaning of the KMES by taking the derivative of Equation 34 and dividing by $I(t)$. Then, using Equation 23 we obtain,

$$\frac{1}{I(t)}\frac{dI(t)}{dt} = K_{\mathrm{T}}\frac{I(t)}{N(t)} - \frac{K_{\mathrm{T}}}{P_c} = K_T - \frac{R(t)}{N(t)}K_T - \frac{K_{\mathrm{T}}}{P_c}. \qquad \text{(S1-5)}$$

The left-hand side of Equation S1-5 is the rate of change of infections per infectious person. Since $K_T = \frac{dN(t)}{dt}\frac{1}{I(t)}$, and is the rate at which infectious persons cause new infections, the terms $-\frac{R(t)}{N(t)}K_T - \frac{K_{\mathrm{T}}}{P_c}$ must be the rate of recovery per infectious person, $\frac{dR(t)}{dt}\frac{1}{I(t)}$.

Finally, we can use Equations 35, and 23 to write this simple expression for the solution for total cases if $K_T(t)$ and $P_c(t)$ remain constant:

$$N(t) = N_\infty^{(1-F_i(t))}. \qquad \text{(S1-6)}$$

where $F_i(t) = \frac{I(t)}{N(t)} = e^{-\frac{K_T}{P_c}t}$ and is the fraction infected.

Supplement 2. Controlling epidemics early

The quantitative mathematical relationships derived from the KMES in Section 1 characterize the dynamics of an epidemic and illustrate that strong and early intervention is critical. Equation 38 quantifies that the ultimate number of individuals infected in an epidemic, N_∞, will be exponentially dependent on the number of people with whom each person interacts.

The real-world country data provide vivid examples of the consequences projected by the KMES. Both South Korea and New Zealand enacted strong and early interventions compared to other countries (Campbell, C 2020; Field, A 2020), as reflected by their $\frac{K_T}{P_c}$ values (Table 2). These strong interventions led to earlier peaks in new cases and to far fewer total cases than in other countries (Figures 4 and 5) in the first few months of the pandemic: the peak number of new cases in both South Korea and New Zealand was 90–99% lower than in other countries, a compelling validation of the explicit statement in the KMES that strong intervention leads to *exponentially* more favorable outcomes.

In the USA, interventions initiated on March 16 began to have an effect around March 23, 2020 (Figure 4B); the number of active cases on March 23, 2020 (Roser et al 2021) was 46,136. Using the values of $\ln\left(F_i(0)K_T(\mathrm{t})\right)$ and $\frac{K_T}{P_c}$ calculated from the data, Equation 38 predicts that the ultimate number of cases would have been approximately 1.22 million. If the same intervention had been implemented and sustained starting on March 10, when there were 59 times fewer (782) cases (Roser et al 2021), the model predicts that the ultimate number of

cases would also have been 59 times lower, or 20,725. Thus, earlier action could have reduced the ultimate number of projected cases by more than 98%. Of course, the projected estimate of approximately 1.22 million total USA cases would only have occurred if the effectiveness of the interventions that were launched on March 16 had been sustained. Unfortunately, a marked reduction in effective interventions occurred in many parts of the USA in mid-April, well before the official reopening of the economy (Elassar 2020). This caused a second surge in new cases in late April and is why the observed data and the model prediction diverge in Figure 4B.

As shown in the main body of the paper, Section 1, the KMES provides an estimate of the time to the peak of new cases, $t_{\max}$. Using Equation 42 and the values of $\ln\left(F_i(0)K_T(\mathrm{t})\right)$ and $\frac{K_T}{P_c}$ calculated from the data, the predicted peak in new cases in the USA would have occurred near March 24 if the intervention had begun on March 10. Instead, a 6-day delay in effective intervention shifted the initial peak to April 11, 16 days later, as projected, and that peak was much higher (Figure 4B).

As shown, too, in Section 3, epidemic acceleration, the instantaneous potential to change the pace of the epidemic, can be determined at any point in the epidemic and depends on the social containment actions in effect at that time. What is perhaps less apparent, but predicted by the KMES, is that two countries with identical numbers of cases on a given day can, in fact, have different accelerations on the same day, and will, therefore, exhibit different dynamics immediately after that day.

South Korea and New Zealand (Figure 4A and F) had nearly identical case counts when each imposed strong containment measures (204 cases in South Korea on February 21, and 205 in New Zealand on March 25). Their models suggest that their interventions were about similarly effective ($\frac{K_T}{P_c}$ = 0.22 in South Korea and 0.12 in New Zealand; see Table 2). However, since South Korea has a much higher population density than New Zealand ((Worldometers 2021), data in Table 1), it had a much higher number of interactions when the interventions were imposed and, therefore, a higher rate of acceleration, as evidenced by its higher RCO at the time of intervention. Indeed, the rate of change of new cases *was* higher in South Korea than in New Zealand, and the later number of cases in South Korea *was* higher than in New Zealand (Figure 4A and F).

Equation 42 clearly illustrates these lessons. As social distancing is strengthened (lower P_c), the Effective Replication Number decreases, and the epidemic slows. Early and strong interventions, especially in countries with indigenously high levels of social interaction, are necessary to stop an epidemic in the initial stages. Reopening, enacted too early, can reignite the epidemic, dramatically increasing the number of cases. The astonishing magnitude of the effects, driven by only a few days of delay, derives from the doubly exponential nature of the underlying relationships.

Supplement 3. Ending an Ongoing Epidemic

We can use the KMES to design measures to end an epidemic in an advanced stage. The management plan is built by first using Equation 62 to predict the number of days a given level of intervention, $\frac{K_T}{P_c}$, is needed to reduce the new daily cases by a target fraction, D_{tf}.

For example, using Equation 62, we see that a country targeting a 90% reduction of new cases per day (e.g., from 50,000 to 5,000 cases per day, $D_{tf} = 0.1$), can attain its target in about 12 days by imposing a containment level of $\frac{K_T}{P_c} = 0.2$. The South Korea and New Zealand data demonstrate that Equation 62 is valid and that $\frac{K_T}{P_c} = 0.2$ is achievable for this duration. Both countries achieved a value of $\frac{K_T}{P_c}$ close to 0.2 for the time necessary to produce a 90% reduction. It took 13 days for South Korea (March 3–16) and 15 days for New Zealand (April 2–15) to reduce their new cases by 90% between the dates shown.

Returning to the planning example, after achieving the initial 90% reduction, a reasonable next step might be to relax social containment to a level that allows the economy to remain viable, while preventing the epidemic from erupting again. We can again find the level of $\frac{K_T}{P_c}$ necessary to achieve a chosen target, using Equation 62. If an additional 90% reduction in new cases per day is desired, and a period of 90 days is tolerable for that reduction, then a new level of approximately $\frac{K_T}{P_c} = 0.026$ is needed. This equates to a 90-day period during which each

person can be in contact with seven specific people, in an infectable way. Note that this is three times *less* stringent than the original USA shutdown level in April 2020 as shown by the level of $\frac{K_T}{P_c}$ calculated for the United States in that period (Table 2). Thus, with a well-planned approach, a country can reduce its new daily cases by 99% in approximately 100 days, enabling the country to control, and essentially end the epidemic, while simultaneously maintaining economic viability.

If even 0.026 is too restrictive, we can choose a still lower $\frac{K_T}{P_c}$, but it must be large enough to avoid a new outbreak. A lower bound for the new value of $\frac{K_T}{P_c}$, high enough to prevent an outbreak, can be found using Equation 54.

We can easily monitor the progress of interventions using the RCO, as the curve for South Korea illustrates (Figure 4A). Had this country maintained the implemented level of distancing measures, the data would have followed the initial slope. However, the actual data departed from the slope, heralding failures in (or relaxation of) social distancing, which were later documented to have occurred during the indicated time frame (Campbell 2020) (circled data, Figure 4A). Because it summarizes epidemic dynamics, we can use the RCO to continuously determine the effectiveness of implemented measures and whether they need adjustment.

Supplement 3.1 Outbreaks

We can see from Equation 51 that if the social interventions are strengthened (lower P_c) the slope of the RCO curve will steepen and if the interventions are relaxed, the slope will become shallower. Therefore, if the value of $K_T(t)$ does not change due to a change in the disease transmissibility, the RCO is a metric for monitoring the population interactions. It is also clear that under the assumptions used to develop the KMES, $\frac{K_T}{P_c}$ must always be greater than zero, and the RCO slope can never become positive. However, this only remains true if these three conditions remain true: 1) immunity persists, 2) no new infections are introduced from outside the area, 3) $\Delta P_{cni}(n\Delta t)$ is a much smaller order of magnitude than the new infections, $K_T(n\Delta t)\Delta t$. We call the latter two conditions the assumption that the epidemic is contiguous.

If new infections are introduced into a portion of the population that has thus far been disconnected from the previously infected area, and therefore, has only susceptible people, then the assumption of contiguousness does not hold. This is a common situation when infected people travel from an infected area to a previously uninfected area and cause an outbreak.

In this case, we will begin with Equation 22 and assume that the entirety of the change in $P_c(t)$ during the time Δt is with uninfected new contacts. That is, $\Delta P_c(t) = \Delta P_{cni}(t)$; and Equation 22 becomes,

$$\frac{I(n\Delta t)}{N(n\Delta t)} = \left(1 - \frac{K_T(0)\Delta t - \Delta P_c(0)}{P_c(0)}\right)\left(1 - \frac{K_T(\Delta t)\Delta t - \Delta P_c(\Delta t)}{P_c(\Delta t)}\right)\ldots\left(1 - \frac{K_T(n\Delta t)\Delta t - \Delta P_c(n\Delta t)}{P_c(n\Delta t)}\right) \tag{S3-1}$$

and then, since by definition, $n\Delta t = t$, as $n \to \infty, \Delta t \to 0$, Equation S3-4 becomes,

$$\frac{I(t)}{N(t)} = F_i(0)e^{-\int_0^t \frac{K_T(t) - \frac{dP_c(t)}{dt}}{P_c(t)}dt} = F_i(0)\frac{P_c(t)}{P_c(0)}e^{-\int_0^t \frac{K_T(t)}{P_c(t)}dt} \tag{S3-2}$$

The equations for $N(t), I(t)$, and $R(t)$ are then the following:

$$N(t) = N(0)e^{F_i(0)\int_0^t K_T(t)\frac{P_c(t)}{P_c(0)}e^{-\int_0^t \frac{K_T(a)}{P_c(a)}da}dt} \tag{S3-3}$$

$$I(t) = I(0)\frac{P_c(t)}{P_c(0)}e^{F_i(0)\int_0^t K_T(t)\frac{P_c(t)}{P_c(0)}e^{-\int_0^t \frac{K_T(a)}{P_c(a)}da}dt - \int_0^t \frac{K_T(t)}{P_c(t)}dt} \tag{S3-4}$$

$$R(t) = (N(0) - I(0)\frac{P_c(t)}{P_c(0)}e^{-\int_0^t \frac{K_T(t)}{P_c(t)}dt})e^{F_i(0)\int_0^t K_T(t)\frac{P_c(t)}{P_c(0)}e^{-\int_0^t \frac{K_T(a)}{P_c(a)}da}dt} \tag{S3-5}$$

As an alternative, to predict the number of cases in an epidemic affected by an outbreak, we can modify Equation 35. Assuming that $t_0 = 0$, $N(0) = 1$, and introducing the notation P_{cx} where x denotes the number of the outbreak, Equation 35 can be written as:

$$N(t) = e^{-P_{c1}(e^{-\frac{K_T}{P_{c1}}t} - 1)}. \tag{S3-6}$$

If a new outbreak occurs in a previously unaffected area of a country, then Equation S3-6 can be modified as follows:

$$N(t) = e^{-P_{c1}(e^{-\frac{K_T}{P_{c1}}\mathrm{t}}-1)} + I_2 e^{-P_{c2}(e^{-\frac{K_T}{P_{c2}}(\mathrm{t}-t_2)}-1)}, \quad \text{(S3-7)}$$

where I_2 is the number of infectious people who initiated the new outbreak, P_{c2} is the social interaction parameter in the new outbreak area, and t_2 is the time the new outbreak occurs. We have assumed that the disease transmissibility remains the same throughout this illustration. If the transmissibility changes in a subset of the population, then a similar formulation, using the notation, K_{Tx}, can be utilized to track the populations with the new transmissibility.

Equation S3-7 can be written in a general form as

$$N(t) = e^{-P_{c1}(e^{-\frac{K_T}{P_{c1}}\mathrm{t}}-1)} + I_2 e^{-P_{c2}(e^{-\frac{K_T}{P_{c2}}(\mathrm{t}-t_2)}-1)} \ldots + I_{\mathrm{x}} e^{-P_{cx}(e^{-\frac{K_T}{P_{cx}}(\mathrm{t}-t_x)}-1)}, \quad \text{(S3-8)}$$

where x denotes the outbreak number and $\mathrm{t} > t_2 > t_3 > \cdots > t_x$. For each outbreak t_x, P_{cx}, and I_x need to be determined independently.

While an epidemic is underway, we can detect an outbreak by monitoring the slope of the RCO curve. A positive slope detected in an RCO curve indicates that an outbreak has occurred. This is an indication that immediate action, within days, is required from policy makers to strengthen intervention measures and prevent the outbreak from overwhelming prior progress in controlling the epidemic.

By monitoring the RCO curve, we can also detect if the disease changes its transmissibility through mutation. In this situation, a proper fit of the parameters in Equation 35 is not possible and a modification of K_T is required to accommodate the change.

Supplement 4: Understanding Kermack and McKendrick's Arrays

The Kermack and McKendrick model can be visually represented in discrete form as arrays of $N(t,\theta), I(t,\theta), R(t,\theta)$ and their derivatives depicted over t and θ according to this array:

(t,0)	(t,Δt)	(t,2Δt)	⋯	(t,t-Δt)	(t,t)
(t-Δt,0)	(t-Δt,Δt)	(t-Δt,2Δt)	⋯	(t-Δt,t-Δt)	(t-Δt,t)
⋮	⋮	⋮	⋯	⋮	⋮
(3Δt,0)	(3Δt,Δt)	(3Δt,2Δt)	⋯	(3Δt,t-Δt)	(3Δt,t)
(2Δt,0)	(2Δt,Δt)	(2Δt,2Δt)	⋯	(2Δt,t-Δt)	(2Δt,t)
(Δt,0)	(Δt,Δt)	(Δt,2Δt)	⋯	(Δt,t-Δt)	(Δt,t)
(0,0)	(0,Δt)	(0,2Δt)	⋯	(0,t-Δt)	(0,t)

Kermack and McKendrick's concept of θ imagined that the time history of the epidemic was a square t by t array with each row representing an increment of time, Δt, and each column representing the progress of a θ group through time. In this conceptualization, each θ group starts at time $t - \theta$ and progresses diagonally upward and to the right through the array. This formulation of the problem also means that θ has the units of time, $d\theta = dt.$, and $\Delta t = \Delta\theta$. Therefore, Δt and $\Delta\theta$ are used interchangeably throughout the array.

Keeping this convention, we can use Equation 2 and the knowledge that $\Delta N(t,\theta) = 0$ when $\theta > 0$ to write the matrix for $\Delta N(t,\theta)$,

$$\Delta N(t,\theta) = \begin{vmatrix} K_T(t-\Delta t)\sum_{\theta=0}^{t-\Delta t} I(t-\Delta t,\theta)\Delta t & 0 & 0 & \cdots & 0 & 0 \\ K_T(t-2\Delta t)\sum_{\theta=0}^{t-\Delta t} I(t-2\Delta t,\theta)\Delta t & 0 & 0 & \cdots & 0 & 0 \\ \vdots & \vdots & \vdots & \cdots & \vdots & \vdots \\ K_T(2\Delta t)\sum_{\theta=0}^{t-\Delta t} I(2\Delta t,\theta)\Delta t & 0 & 0 & \cdots & 0 & 0 \\ K_T(\Delta t)\sum_{\theta=0}^{t-\Delta t} I(\Delta t,\theta)\Delta t & 0 & 0 & \cdots & 0 & 0 \\ K_T(0)\sum_{\theta=0}^{t-\Delta t} I(0,\theta)\Delta t & 0 & 0 & \cdots & 0 & 0 \\ N(0) & 0 & 0 & \cdots & 0 & 0 \end{vmatrix}$$

The arrays for $\Delta R(t,\theta)$, $\Delta I(t,\theta)$, and $I(t,\theta)$ can be written in an identical fashion,

$$\Delta R(t,\theta)=\begin{vmatrix} 0 & \psi(t-\Delta t,0)I(t-\Delta t,0)\Delta t & \psi(t-\Delta t,\Delta t)I(t-\Delta t,\Delta t)\Delta t & \cdots & \psi(t-\Delta t,t-2\Delta t)I(t-\Delta t,t-2\Delta t)\Delta t & \psi(t-\Delta t,t-\Delta t)I(t-\Delta t,t-\Delta t)\Delta t \\ 0 & \psi(t-2\Delta t,0)I(t-2\Delta t,0)\Delta t & \psi(t-2\Delta t,\Delta t)I(t-2\Delta t,\Delta t)\Delta t & \cdots & \psi(t-2\Delta t,t-2\Delta t)I(t-2\Delta t,t-2\Delta t)\Delta t & 0 \\ \vdots & \vdots & \vdots & \cdots & \vdots & \vdots \\ 0 & \psi(2\Delta t,0)I(2\Delta t,0)\Delta t & \psi(2\Delta t,\Delta t)I(2\Delta t,\Delta t)\Delta t & \cdots & 0 & 0 \\ 0 & \psi(\Delta t,0)I(\Delta t,0)\Delta t & \psi(\Delta t,\Delta t)I(\Delta t,\Delta t)\Delta t & \cdots & 0 & 0 \\ 0 & \psi(0,0)I(0,0)\Delta t & 0 & \cdots & 0 & 0 \\ 0 & 0 & 0 & \cdots & 0 & 0 \end{vmatrix}$$

$$\Delta I(t,\theta)=\begin{vmatrix} K_T(t-\Delta t)\sum_{\theta=0}^{t-\Delta t} I(t-\Delta t,\theta)\Delta t & -\psi(t-\Delta t,0)I(t-\Delta t,0)\Delta t & -\psi(t-\Delta t,\Delta t)I(t-\Delta t,\Delta t)\Delta t & \cdots & -\psi(t-\Delta t,t-2\Delta t)I(t-\Delta t,t-2\Delta t)\Delta t & -\psi(t-\Delta t,t-\Delta t)I(t-\Delta t,t-\Delta t)\Delta t \\ K_T(t-2\Delta t)\sum_{\theta=0}^{t-\Delta t} I(t-2\Delta t,\theta)\Delta t & -\psi(t-2\Delta t,0)I(t-2\Delta t,0)\Delta t & -\psi(t-2\Delta t,\Delta t)I(t-2\Delta t,\Delta t)\Delta t & \cdots & -\psi(t-2\Delta t,t-2\Delta t)I(t-2\Delta t,t-2\Delta t)\Delta t & 0 \\ \vdots & \vdots & \vdots & \cdots & \vdots & \vdots \\ K_T(2\Delta t)\sum_{\theta=0}^{t-\Delta t} I(2\Delta t,\theta)\Delta t & -\psi(2\Delta t,0)I(2\Delta t,0)\Delta t & -\psi(2\Delta t,\Delta t)I(2\Delta t,\Delta t)\Delta t & \cdots & 0 & 0 \\ K_T(\Delta t)\sum_{\theta=0}^{t-\Delta t} I(\Delta t,\theta)\Delta t & -\psi(\Delta t,0)I(\Delta t,0)\Delta t & -\psi(\Delta t,\Delta t)I(\Delta t,\Delta t)\Delta t & \cdots & 0 & 0 \\ K_T(0)\sum_{\theta=0}^{t-\Delta t} I(0,\theta)\Delta t & -\psi(0,0)I(0,0)\Delta t & 0 & \cdots & 0 & 0 \\ N(0) & 0 & 0 & \cdots & 0 & 0 \end{vmatrix}$$

$$I(t,\theta)=\begin{vmatrix} K_T(t-\Delta t)\sum_{\theta=0}^{t-\Delta t} I(t-\Delta t,\theta)\Delta t & I(t\text{-}\Delta t,0)(1\text{-}\psi(t\text{-}\Delta t,0)\Delta t) & I(t\text{-}\Delta t,\Delta t)(1\text{-}\psi(t\text{-}\Delta t,\Delta t)\Delta t) & \cdots & I(t\text{-}\Delta t,t\text{-}2\Delta t)(1\text{-}\psi(t\text{-}\Delta t,t\text{-}2\Delta t)\Delta t) & I(t\text{-}\Delta t,t\text{-}\Delta t)(1\text{-}\psi(t\text{-}\Delta t,t\text{-}\Delta t)\Delta t) \\ K_T(t-2\Delta t)\sum_{\theta=0}^{t-\Delta t} I(t-2\Delta t,\theta)\Delta t & I(t\text{-}2\Delta t,0)(1\text{-}\psi(t\text{-}2\Delta t,0)\Delta t) & (t\text{-}2\Delta t,\Delta t)(1\text{-}\psi(t\text{-}2\Delta t,\Delta t)\Delta t] & \cdots & (t\text{-}2\Delta t,t\text{-}2\Delta t)(1\text{-}\psi(t\text{-}2\Delta t,t\text{-}2\Delta t)\Delta t] & 0 \\ \vdots & \vdots & \vdots & \cdots & \vdots & \vdots \\ K_T(2\Delta t)\sum_{\theta=0}^{t-\Delta t} I(2\Delta t,\theta)\Delta t & I(2\Delta t,0)(1\text{-}\psi(2\Delta t,0)\Delta t) & I(2\Delta t,\Delta t)(1\text{-}\psi(2\Delta t,\Delta t)\Delta t) & \cdots & 0 & 0 \\ K_T(\Delta t)\sum_{\theta=0}^{t-\Delta t} I(\Delta t,\theta)\Delta t & I(\Delta t,0)(1\text{-}\psi(\Delta t,0)\Delta t) & I(\Delta t,\Delta t)(1\text{-}\psi(\Delta t,\Delta t)\Delta t) & \cdots & 0 & 0 \\ K_T(0)\sum_{\theta=0}^{t-\Delta t} I(0,\theta)\Delta t & I(0,0)(1\text{-}\psi(0,0)\Delta t) & 0 & \cdots & 0 & 0 \\ N(0) & 0 & 0 & \cdots & 0 & 0 \end{vmatrix}$$

It is clear from this notation that $\Delta I(t,\theta) = \Delta N(t,\theta) - \Delta R(t,\theta)$; and it is interesting to note that $\frac{\Delta N(t,\theta)}{I(t)}$ and $\frac{\Delta R(t,\theta)}{I(t)}$ are, respectively, impulse and step functions in θ.

We now use the preceding arrays to rederive Equation 4. We start with Equation 7,

$$I(t) = \int_0^t B(t,\theta)\frac{dN(t-\theta,0)}{dt}d\theta + B(t,t)I(0), \qquad \text{(S4-1,7)}$$

Our goal is to transform Equation S4-1 to Equation 4 to demonstrate that the arrays are a formulation of the Kermack and McKendrick equations.

Referring to the $I(t,\theta)$ array and keeping in mind that the value of $I(t,0)$ is the value in the $(t,0)$ place in both the $\Delta N(t,\theta)$ and $I(t,\theta)$ arrays, $I(0,0) = N(0) = I(0)$ as shown in the array, $\Delta t = \Delta\theta$, $\frac{dN(t,0)}{dt} = I(t,0)$, $B(\theta) = B(t,\theta)$, and $B(\theta,\theta) = B(t,t)$, we know that,

$$I(t) = \sum_{\theta=0}^{t} I(t,\ \theta) = \sum_{\theta=0}^{t} B(t,\theta) I(t-\theta,0). \tag{S4-2}$$

Equation S4-2 is merely the summation form of S4-1. We use the reference to the $I(t,\theta)$ matrix to show where it comes from in the (t,θ) matrices.

Keeping in mind that ψ is only a function of t, it is also clear from the $I(t,\theta)$ matrix that,

$$I(t) = K_T(t-\Delta t)\Delta t \sum_{\theta=0}^{t-\Delta t} I(t-\Delta t,\ \theta) + (1-\psi(t-\Delta t)\Delta t) \sum_{\theta=0}^{t-\Delta t} I(t-\Delta t,\ \theta) \tag{S4-3}$$

This operation can be repeated all the way back through the matrix to finally obtain the expression,

$$I(t) = (K_T(t-\Delta t)\Delta t + 1 - \psi(t-\Delta t)\Delta t)(K_T(t-2\Delta t)\Delta t$$

$$+1 - \psi(t-2\Delta t)\Delta t) \ldots (K_T(0)\Delta t + 1 - \psi(0)\Delta t) I(0) \tag{S4-4}$$

Equating 46-4 with S4-1 and taking the limit as $\Delta t = \Delta\theta$ go to zero, we arrive at the expression,

$$I(t) = \int_0^t B(t,\theta)\frac{dN(t-\theta,0)}{dt}d\theta + B(t)I(0) = e^{\int_0^t (K_T(t)-\psi(t))dt}I(0) = e^{\int_0^t K_T(t)dt}B(t)I(0) \quad \text{(S4-5)}$$

which is identical to Equation 4 with $\psi(t) = \mu(t)$. The same approach can be used on the arrays for $\Delta N(t,\theta)$ and $\Delta R(t,\theta)$ to find expressions for $\frac{dN(t)}{dt}$ and $\frac{dR(t)}{dt}$ from which the rest of the solution can be determined.

Supplement 5: List of Equations

$$\frac{dS(t)}{dt} = -\frac{dN(t)}{dt} = -\Lambda(t)S(t), \quad (1)$$

$$-\frac{dS(t)}{dt} = \frac{dN(t)}{dt} = K_T(t)I(t), \quad (2)$$

$$\frac{dI(t)}{dt} = (K_T(t) - \mu(t))I(t), \quad (3)$$

$$I(t) = I(0)e^{\int_0^t (K_T(b)-\mu(b))db}. \quad (4)$$

$$N(t) = \int_0^t K_T(\mathrm{c})\mathrm{I}(0)\, e^{\int_0^c (K_T(b)-\mu(b))db}dc \quad (5)$$

$$\frac{dS(t)}{dt} = -\frac{\mathrm{S(t)}}{A_p}\left(\int_0^t A(t,\theta)\frac{dN(t-\theta,0)}{dt}d\theta + A(t,t)I(0)\right), \quad (6)$$

$$I(t) = \int_0^t B(t,\theta)\frac{dN(t-\theta,0)}{dt}d\theta + B(t,t)I(0), \quad (7)$$

$$\frac{dR(t)}{dt} = \int_0^t C(t,\theta)\frac{dN(t-\theta,0)}{dt}d\theta + C(t,t)I(0), \quad (8)$$

$$N(t) = I(t) + R(t) \tag{9}$$

$$N_P - S(t) = N(t) \tag{10}$$

$$\frac{dS(t)}{dt} = -\frac{dN(t)}{dt} \tag{11}$$

$$K_T(t) = -\frac{\frac{dS(t)}{dt}}{I(t)} = \frac{\mathrm{S(t)}(\int_0^t A(t,\theta)\frac{dN(t-\theta,0)}{dt}d\theta + A(t,t)I(0))}{A_P(\int_0^t B(t,\theta)\frac{dN(t-\theta,0)}{dt}d\theta + B(t,t)I(0))}. \tag{12}$$

$$\mu(t) = \frac{\frac{dR(t)}{dt}}{I(t)} = \frac{\int_0^t C(t,\theta)\frac{dN(t-\theta,0)}{dt}d\theta + C(t,t)I(0)}{\int_0^t B(t,\theta)\frac{dN(t-\theta,0)}{dt}d\theta + B(t,t)I(0)}. \tag{13}$$

$$-\frac{dS(t)}{dt} = \frac{dN(t)}{dt} = \mathrm{K}_T(t)\, I(t), \tag{14}$$

$$\frac{dI(t)}{dt} = K_T(t)\, I(t) - \mu(t)\, I(t), \tag{15}$$

$$\frac{dR(t)}{dt} = \mu(t)I(t) \text{ and} \tag{16}$$

$$S(t) = N_P - N(t), \tag{17}$$

$$P_c(t) = \lim_{\Delta t \to 0} \int_t^{t+\Delta t} P_{cr}(t)dt, \tag{18}$$

$$I(\Delta t) = N(\Delta t) - \frac{K_T(0)\Delta t - \Delta P_{cni}(0)}{P_c(0)} N(\Delta t). \tag{19}$$

$$\frac{I(\Delta t)}{N(\Delta t)} = 1 - \frac{K_T(0)\Delta t - \Delta P_{cni}(0)}{P_c(0)} \tag{20}$$

$$\frac{I(2\Delta t)}{N(2\Delta t)} = (1 - \frac{K_T(0)\Delta t - \Delta P_{cni}(0)}{P_c(0)})(1 - \frac{K_T(\Delta t)\Delta t - \Delta P_{cni}(\Delta t)}{P_c(\Delta t)}). \tag{21}$$

$$\frac{I(t)}{N(t)} = F_i(0)e^{-\int_0^t \frac{K_T(t)}{P_c(t)}dt}, \tag{23}$$

$$N(t) = N(0)e^{\int_0^t K_T(t)\frac{I(t)}{N(t)}dt}. \tag{24}$$

$$N(t) = N(0)e^{F_i(0)\int_0^t K_T(t)e^{-\int_0^t \frac{K_T(a)}{P_c(a)}da}dt}. \tag{25}$$

$$I(t) = I(0)e^{F_i(0)\int_0^t K_T(t)e^{-\int_0^t \frac{K_T(a)}{P_c(a)}da}dt-\int_0^t \frac{K_T(t)}{P_c(t)}dt}, \tag{26}$$

$$R(t) = (N(0) - I(0)e^{-\int_0^t \frac{K_T(t)}{P_c(t)}dt})e^{F_i(0)\int_0^t K_T(t)e^{-\int_0^t \frac{K_T(a)}{P_c(a)}da}dt}. \tag{27}$$

$$B(t,\theta) = e^{-\int_{t-\theta}^t \psi(t,a)da} = e^{-\int_{t-\theta}^t (K_T(a)-F_i(0)K_T(a)e^{-\int_0^a \frac{aK_T(b)}{P_c(b)}db}+\frac{K_T(a)}{P_c(a)})da} \tag{28}$$

$$B(t,t) = e^{-\int_0^t \psi(t,a)da} = e^{-\int_0^t (K_T(a)-F_i(0)K_T(a)e^{-\int_0^a \frac{aK_T(b)}{P_c(b)}db}+\frac{K_T(a)}{P_c(a)})da} \tag{29}$$

$$\mu(t) = \psi(t,\theta) = \frac{\frac{dR(t)}{dt}}{I(t)} = K_T(t)-F_i(0)K_T(t)e^{-\int_0^t \frac{K_T(t)}{P_c(t)}dt} + \frac{K_T(t)}{P_c(t)} \tag{30}$$

$$\varphi(t,\theta) = \frac{K_T(t)A_p}{S(t)} \tag{31}$$

$$I(t) = e^{\int_0^t K_T(t)dt}B(t,t)I(0) \tag{32}$$

$$N(t) = e^{\int_0^t (K_T(t)+\frac{K_T(t)}{P_c(t)})dt}B(t,t)\frac{I(0)}{F_i(0)} \tag{33}$$

$$R(t) = (\frac{e^{\int_0^t (K_T(t)+\frac{K_T(t)}{P_c(t)})dt}}{F_i(0)} - e^{\int_0^t K_T(t)dt})B(t,t)I(0). \tag{34}$$

$$N(t) = N(0)e^{-F_i(0)P_c(e^{-\frac{K_T}{P_c}t}-1)} \tag{35}$$

$$I(t) = I(0)e^{-F_i(0)P_c\left(e^{-\frac{K_T}{P_c}t}-1\right)-\frac{K_T}{P_c}t} \tag{36}$$

$$R(t) = (N(0) - I(0)e^{-\frac{K_T}{P_c}t})e^{-F_i(0)P_c(e^{-\frac{K_T}{P_c}t}-1)} \tag{37}$$

$$N(\infty) = e^{F_i(0)P_c}, \tag{38}$$

$$t = -\frac{P_c}{K_T} ln(1 - \frac{\ln(S(0))}{F_i(0)P_c}) \tag{39}$$

$$F_i(0)P_c > \ln(S(0)). \tag{40}$$

$$R_{Eff} = \frac{1}{1-F_i(0)e^{-\frac{K_T}{P_c}t}+\frac{1}{P_c}}. \tag{41}$$

$$t_{decline} = \frac{P_c \ln(F_i(0)P_c)}{K_T}. \tag{42}$$

$$t_{max} = \frac{P_c \ln(F_i(0)P_c)}{K_T}, \tag{43}$$

$$I(t)_{Peak} = \frac{I(0)e^{(F_i(0)P_c-1)}}{F_i(0)P_c}. \tag{44}$$

$$P_{cr}(\mathrm{t}) = \frac{A_{1r}(t)N_p}{A_p} = contact\ rate, \tag{45}$$

$$A_1(t) = \lim_{\Delta t \to 0} \int_t^{t+\Delta t} A_{1r}(t)dt, \tag{46}$$

$$\frac{K_T(t)}{P_c(t)} = \frac{K_T(t)A_p}{A_1(t)N_p}. \tag{47}$$

$$F(N(t) = \frac{A_1 N_p}{A} \ln\left(1 + \frac{\ln(N(t))}{-\frac{A_1 N_p}{A}}\right) = -K_T \mathrm{t}, \tag{48}$$

$$B(t,t) = e^{-(e^{-K_T t}-1)-2K_T t} \tag{49}$$

$$Viral\ Load = e^{-(e^{-K_T t}-1)-2K_T t}(2 - e^{-K_T t}), \tag{50}$$

$$RCO = ln\left(\frac{\frac{dN(t)}{dt}}{N(t)}\right) = \ln(F_i(0)K_T) - \frac{K_\mathrm{T}}{P_c} t \tag{51}$$

$$P_{cal} = \frac{-K_T(t)}{Slope(1-\frac{G_{R0}}{100})}, \tag{52}$$

$$\frac{dS(t)}{dt} = -\frac{\beta I(t) S(t)}{N_p}, \tag{53}$$

$$\frac{dI(t)}{dt} = \frac{\beta I(t) S(t)}{N_p} - \gamma I(t), \tag{54}$$

$$\frac{dR(t)}{dt} = \gamma I(t), \text{ and} \tag{55}$$

$$N_p = S(t) + I(t) + R(t), \tag{56}$$

$$R_{Eff} = \frac{1}{1-\frac{e^{RCO(t)}}{K_T}+\frac{1}{P_\mathrm{c}}}. \tag{57}$$

$$\frac{d^2N(t)}{d^2t} = \left(K_\mathrm{T} F_i(0) e^{-\frac{K_T}{P_c}t} - \frac{K_T}{P_c}\right)\frac{dN(t)}{dt} = K_T(\frac{I(t)}{N(t)} - \frac{1}{P_c})\frac{dN(t)}{dt} = \left(e^{RCO(t)} - \frac{K_T}{P_c}\right)\frac{dN(t)}{dt} = K_\mathrm{T}\frac{dI(t)}{dt}. \tag{58}$$

$$P_c < K_T e^{-RCO(t)}. \tag{59}$$

$$D_{tf} = \frac{\frac{dN\left(t+t_{target}\right)}{dt}}{\frac{dN(t)}{dt}} = \frac{New\ Case\ Target\ Rate}{Current\ New\ Case\ Rate}, \tag{60}$$

$$D_{tf} = e^{-P_c\left(e^{-\frac{K_T}{P_c}(t+t_{target})} - e^{-\frac{K_T}{P_c}(t)}\right)} e^{-\frac{K_T}{P_c}t_{\text{target}}}. \tag{61}$$

$$t_{target} = -\frac{P_c \ln\left(D_{tf}\right)}{K_T}. \tag{62}$$

$$\frac{d\left(\frac{I(t)}{N(t)}\right)}{dt} = -\frac{K_T(t)I(t)}{P_c(t)N(t)} \tag{23}$$

$$\frac{d\left(\frac{I(t)}{N(t)}\right)}{dt} = \frac{d(I(t)}{dt}\frac{1}{N(t)} - \frac{dN(t)}{dt}\frac{I(t)}{N(t)^2} = -\frac{I(t)}{N(t)}\frac{K_{\mathrm{T}}(t)}{P_c(t)} \tag{S1-2}$$

$$\frac{d\left(\frac{I(t)}{N(t)}\right)}{dt} = \frac{\frac{dI(t)}{dt} - \frac{dN(t)}{dt}\frac{I(t)}{N(t)}}{N(t)} = \frac{-I(t)\frac{K_{\mathrm{T}}(t)}{P_c(t)}}{N(t)} \tag{S1-3}$$

$$\frac{dR(0)}{dt} = I(0)\frac{K_{\mathrm{T}}(0)}{P_c(0)} \tag{S1-4}$$

$$\frac{1}{I(t)}\frac{dI(t)}{dt} = K_{\mathrm{T}}\frac{I(t)}{N(t)} - \frac{K_{\mathrm{T}}}{P_c} = K_T - \frac{R(t)}{N(t)}K_T - \frac{K_{\mathrm{T}}}{P_c}. \tag{S1-5}$$

$$N(t) = N_{\infty}^{(1-F_i(t))}. \tag{S1-6}$$

$$\frac{I(n\Delta t)}{N(n\Delta t)} = \left(1 - \frac{K_T(0)\Delta t - \Delta P_c(0)}{P_c(0)}\right)\left(1 - \frac{K_T(\Delta t)\Delta t - \Delta P_c(\Delta t)}{P_c(\Delta t)}\right)\ldots\left(1 - \frac{K_T(n\Delta t)\Delta t - \Delta P_c(n\Delta t)}{P_c(n\Delta t)}\right) \tag{S3-1}$$

$$\frac{I(t)}{N(t)} = F_i(0)e^{-\int_0^t \frac{K_T(t) - \frac{dP_c(t)}{dt}}{P_c(t)}dt} = F_i(0)\frac{P_c(t)}{P_c(0)}e^{-\int_0^t \frac{K_T(t)}{P_c(t)}dt} \tag{S3-2}$$

$$N(t) = N(0)e^{F_i(0)\int_0^t K_T(t)\frac{P_c(t)}{P_c(0)}e^{-\int_0^t\frac{K_T(a)}{P_c(a)}da}dt} \quad \text{(S3-3)}$$

$$I(t) = I(0)\frac{P_c(t)}{P_c(0)}e^{F_i(0)\int_0^t K_T(t)\frac{P_c(t)}{P_c(0)}e^{-\int_0^t\frac{K_T(a)}{P_c(a)}da}dt-\int_0^t\frac{K_T(t)}{P_c(t)}dt} \quad \text{(S3-4)}$$

$$R(t) = (N(0) - I(0)\frac{P_c(t)}{P_c(0)}e^{-\int_0^t\frac{K_T(t)}{P_c(t)}dt})e^{F_i(0)\int_0^t K_T(t)\frac{P_c(t)}{P_c(0)}e^{-\int_0^t\frac{K_T(a)}{P_c(a)}da}dt} \quad \text{(S3-5)}$$

$$N(t) = e^{-P_{c1}(e^{-\frac{K_T}{P_{c1}}t}-1)}. \quad \text{(S3-6)}$$

$$N(t) = e^{-P_{c1}(e^{-\frac{K_T}{P_{c1}}t}-1)} + I_2e^{-P_{c2}(e^{-\frac{K_T}{P_{c2}}(t-t_2)}-1)}, \quad \text{(S3-7)}$$

$$N(t) = e^{-P_{c1}(e^{-\frac{K_T}{P_{c1}}t}-1)} + I_2e^{-P_{c2}(e^{-\frac{K_T}{P_{c2}}(t-t_2)}-1)} \ldots + I_xe^{-P_{cx}(e^{-\frac{K_T}{P_{cx}}(t-t_x)}-1)}, \quad \text{(S3-8)}$$

$$I(t) = \int_0^t B(t,\theta)\frac{dN(t-\theta,0)}{dt}d\theta + B(t,t)I(0), \quad \text{(S4-1,7)}$$

$$I(t) = \sum_{\theta=0}^{t} I(t,\ \theta) = \sum_{\theta=0}^{t} B(t,\theta)I(t-\theta,0). \quad \text{(S4-2)}$$

$$I(t) = K_T(t-\Delta t)\Delta t\sum_{\theta=0}^{t-\Delta t} I(t-\Delta t,\ \theta) + (1-\psi(t-\Delta t)\Delta t)\sum_{\theta=0}^{t-\Delta t} I(t-\Delta t,\ \theta) \quad \text{(S4-3)}$$

$$I(t) = (K_T(t-\Delta t)\Delta t + 1 - \psi(t-\Delta t)\Delta t)(K_T(t-2\Delta t)\Delta t$$

$$+1-\psi(t-2\Delta t)\Delta t)\ldots(K_T(0)\Delta t + 1 - \psi(0)\Delta t)I(0) \quad \text{(S4-4)}$$

$$I(t) = \int_0^t B(t,\theta)\frac{dN(t-\theta,0)}{dt}d\theta + B(t)I(0) = e^{\int_0^t (K_T(t)-\psi(t))dt} I(0) = e^{\int_0^t K_T(t)dt} B(t)I(0) \quad \text{(S4-5)}$$